REPORT DOCUMENTATION PAGE

Form Approved OMB NO. 0704-0188

1. REPORT DATE (DD-MM-YYYY)	2. REPORT TYPE	3. DATES COVERED (From - To)
07-03-2022	Final Report	1-May-2018 - 30-Oct-2021

4. TITLE AND SUBTITLE
Final Report: A Versatile New Architecture for High-Coherence, Chip-Scale Photonics

5a. CONTRACT NUMBER
W911NF-18-1-0160

5b. GRANT NUMBER

5c. PROGRAM ELEMENT NUMBER
611102

6. AUTHORS

5d. PROJECT NUMBER

5e. TASK NUMBER

5f. WORK UNIT NUMBER

7. PERFORMING ORGANIZATION NAMES AND ADDRESSES
California Institute of Technology
California Institute of Technology
1200 E. California Blvd.
Pasadena, CA 91125 -0001

8. PERFORMING ORGANIZATION REPORT NUMBER

9. SPONSORING/MONITORING AGENCY NAME(S) AND ADDRESS (ES)
U.S. Army Research Office
P.O. Box 12211
Research Triangle Park, NC 27709-2211

10. SPONSOR/MONITOR'S ACRONYM(S)
ARO

11. SPONSOR/MONITOR'S REPORT NUMBER(S)
72805-EL.1

12. DISTRIBUTION AVAILIBILITY STATEMENT
Approved for public release; distribution is unlimited.

13. SUPPLEMENTARY NOTES
The views, opinions and/or findings contained in this report are those of the author(s) and should not contrued as an official Department of the Army position, policy or decision, unless so designated by other documentation.

14. ABSTRACT

15. SUBJECT TERMS

16. SECURITY CLASSIFICATION OF:			17. LIMITATION OF ABSTRACT	15. NUMBER OF PAGES	19a. NAME OF RESPONSIBLE PERSON
a. REPORT	b. ABSTRACT	c. THIS PAGE			Amnon Yariv
UU	UU	UU	UU		19b. TELEPHONE NUMBER 626-395-4821

RPPR Final Report
as of 07-Mar-2022

Agency Code: 21XD

Proposal Number: 72805EL **Agreement Number: W911NF-18-1-0160**
INVESTIGATOR(S):

Name: Amnon Yariv
Email: ayariv@caltech.edu
Phone Number: 6263954821
Principal: Y

Organization: **California Institute of Technology**
Address: California Institute of Technology, Pasadena, CA 911250001
Country: USA
DUNS Number: 009584210 EIN: 951643307

Report Date: 30-Jan-2022 Date Received: 07-Mar-2022

Final Report for Period Beginning 01-May-2018 and Ending 30-Oct-2021
Title: A Versatile New Architecture for High-Coherence, Chip-Scale Photonics
Begin Performance Period: 01-May-2018 **End Performance Period:** 30-Oct-2021
Report Term: 0-Other

Submitted By: Amnon Yariv Email: ayariv@caltech.edu
Phone: (626) 395-4821

STEM Degrees: **STEM Participants:**

Major Goals: See attached report (pdf)

Accomplishments: See attached report (pdf)

Training Opportunities: Nothing to Report

Results Dissemination: Nothing to Report

Honors and Awards: Nothing to Report

Protocol Activity Status:

Technology Transfer: Nothing to Report

PARTICIPANTS:

Participant Type: PD/PI
Participant: Amnon Yariv
Person Months Worked: 1.00 **Funding Support:**
Project Contribution:
National Academy Member: Y

Participant Type: Co PD/PI
Participant: Christos Santis
Person Months Worked: 3.00 **Funding Support:**
Project Contribution:
National Academy Member: N

RPPR Final Report
as of 07-Mar-2022

Participant Type: Technician
Participant: Kevin Cooper
Person Months Worked: 8.00 **Funding Support:**
Project Contribution:
National Academy Member: N

Partners

,

I certify that the information in the report is complete and accurate:
Signature: Amnon Yariv
Signature Date: 3/7/22 4:30PM

A Versatile New Architecture for High-Coherence, Chip-Scale Photonics

Amnon Yariv

Christos T. Santis

Caltech

Army Research Office
Michael Gerhold (PM)
Final Report

Amnon Yariv (PI)
Monday, Mar. 07, 2022
Pasadena, CA

Table of contents

Caltech

Project goals

Caltech

- The primary goal of this effort was the demonstration of electrically driven, semiconductor-based (i.e. III-V) gain, ***directly*** integrated on Silicon Nitride (SiN)

  "Direct" in the above refers to the absence of any third, intermediary material (e.g. Silicon) facilitating the optical interfacing of III-V and SiN

- **Why SiN?**

  SiN is a fast-developing material platform for integrated photonics. It features certain unique advantages, especially as compared to Si

  - Potential for ultra-low optical loss (i.e. absorption, scattering, $< .1\ db/m$ in IR)
  - Good optical non-linearity (third-order $\chi^{(3)}$) combined with practical absence of two-photon absorption (TPA)
  - Very wide optical transparency (from UV to mid-IR)
  - Low thermo-optic coefficient (dn/dT) → relative temperature insensitivity

Technical approach: overview

Caltech

- The main challenge in integrating III-V with SiN *directly* is coupling light from one to the other in an efficient and seamless manner (i.e. low loss, low reflection). This stems from the relatively large difference in refractive index (R.I.) between the two (III-V: > 3, SiN: ~ 2.0). Light tends to prefer the material with the higher R.I., in this case III-V, making light confinement in SiN in the presence of III-V or the efficient exchange of energy between the two quite problematic. This is especially true for the thicker III-V films ($1.0 - 2.0\ \mu m$) typically used in heterogeneous integration (see. Fig. 1a below).
- To overcome this issue, we proposed reducing the overall III-V film thickness by about an order of magnitude (see. Fig. 1b below). In doing so, the effective mode index (n_{eff}) of the III-V waveguide decreases to a point where phase-matching with the SiN mode, enabling high-ideality coupling.
- Further, for the efficient and low-(optical) loss electrical driving of the ultra-thin III-V, we proposed the formation of a buried active region (QW) and its lateral injection with carriers.

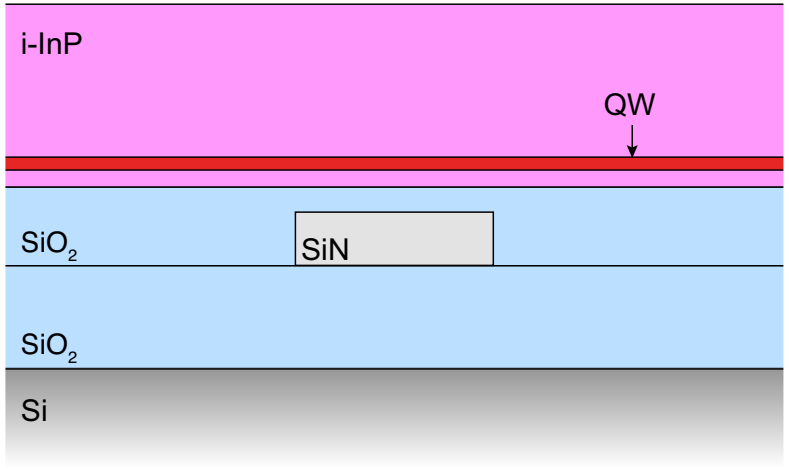

Fig. 1a

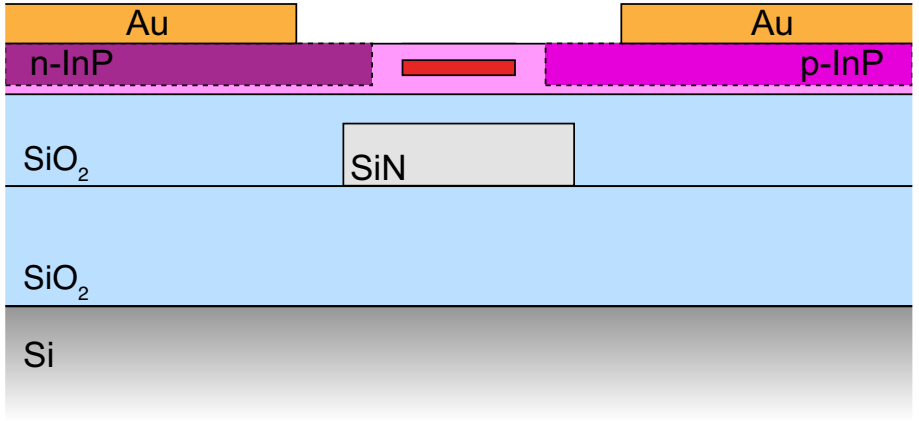

Fig. 1b

Demonstrators

Caltech

As proof-of-concept of the direct integration of III-V gain on SiN using the proposed technical approach, we defined two demonstrators:

- **Narrow-linewidth laser**

The potential for linewidth reduction stems from the low loss in SiN, leveraged through the incorporation, either internally or externally, of a high-Q resonator in the laser cavity . Depending on the configuration, the resonator can be used to either store optical energy or to provide instantaneous negative feedback (i.e. corrections) to laser phase and frequency fluctuations

Target metrics set for the laser:

- < 100 Hz (Lorentzian linewidth)
- >20 mW output power

- **On-chip-powered optical parametric oscillator**

Harnessing SiN's low loss and optical nonlinearity, multiple optical frequencies can be generated non-linearly using only a single frequency as an input (i.e. pump) provided by the on-chip III-V gain. Special case of this kind of parametric oscillator is a frequency comb, where a large number of spectrally equidistant and spanning a relatively broad spectrum is generated.

SiN wafers

Caltech

- One of the first and most important choices was that of SiN and the procurement of wafers
- The first factor was that of optical quality (i.e. low loss). Stoichiometric SiN (Si_3N_4) deposited via low-pressure, chemical vapor deposition (LPCVD) is the highest quality SiN
- The second factor was that of thickness. Aiming for a nonlinear demonstration based on four-wave mixing (FWM), the thickness had to be such that phase-matching, through engineering of the group velocity, could be achieved. For a center wavelength (i.e. pump) of 1.55 um, that meant a SiN thickness of $\sim 800\ nm$.
- Stoichiometric SiN features high tensile stress, making films thicker than about $400\ nm$ difficult to obtain due to cracking. At present, only a handful of commercial or academic foundries, capable of producing Si_3N_4 thicker than $400\ nm$, exist. One of them is Ligentec S.A., a commercial foundry based out of Lausanne, Switzerland and with a proven record of high-quality films. Ligentec was our first choice for SiN wafers. In addition to the deposition of the material to the requisite thickness ($800\ nm$), their services included lithography, cladding (i.e. top) and planarization (CMP).
- Unfortunately, upon receipt, it soon became clear that the Ligentec material could not be used with a high degree of confidence. Specifically, MIT-LL determined that they could not bond to it with high enough yield. The most probable theory is that that was due to a remaining topography on the surface of the wafers (post-CMP), a possible artifact of Ligentec's proprietary method of depositing thick Si_3N_4.
- At that point, we decided to drop the Ligentec material and instead use MIT-LL's in-house Si_3N_4. MIT-LL had already demonstrated the ability to bond to their own wafers with acceptable yields. The downside was MIT-LL's Si_3N_4 was limited to a maximum thickness of $400\ nm$, largely for the reasons explained above. The decision to switch from a $800\ nm$ to a $400\ nm$-thick Si_3N_4 meant that the nonlinear demonstrator could no longer be pursued.

Thermal modeling

Caltech

- For efficient optical power generation, it is critical that heating in the III-V is managed effectively. This is especially true for heterogeneous platforms made of low thermal conductivity materials (e.g. SiO_2, SiN). All other things equal, heating is expected to be more pronounced for the ultra-thin III-V employed in this project, owing to reduced sheet resistance.
- **To offset the increase of resistive heating due to increased sheet resistance, we increase the length of the active region**.
- To understand exactly how the ultra-thin III-V heats up as well as its magnitude, we carried out a rigorous modeling of heat transfer using the finite element method (COMSOL).

Thermal modeling

Caltech

- On the right is an example of a heat transfer simulation for a 200 nm-thick III-V sitting on top of a 4 um-thick SiO_2. The length of the III-V is 6 mm and driven with a current of 500 mA. On the far right is the full simulation domain, that includes a ~500 um-thick Si substrate. T
- The result of the simulation is a 2D map of the temperature rise across the structure, relative to a reference temperature. The latter corresponds to the temperature of the backside of the chip, which is kept fixed via a TEC.
- Red arrows represent the direction and magnitude of heat flux. It is evident that heat escapes from the active region (QW) primarily along the metal electrodes (Au), owing to the metal's high thermal conductivity.

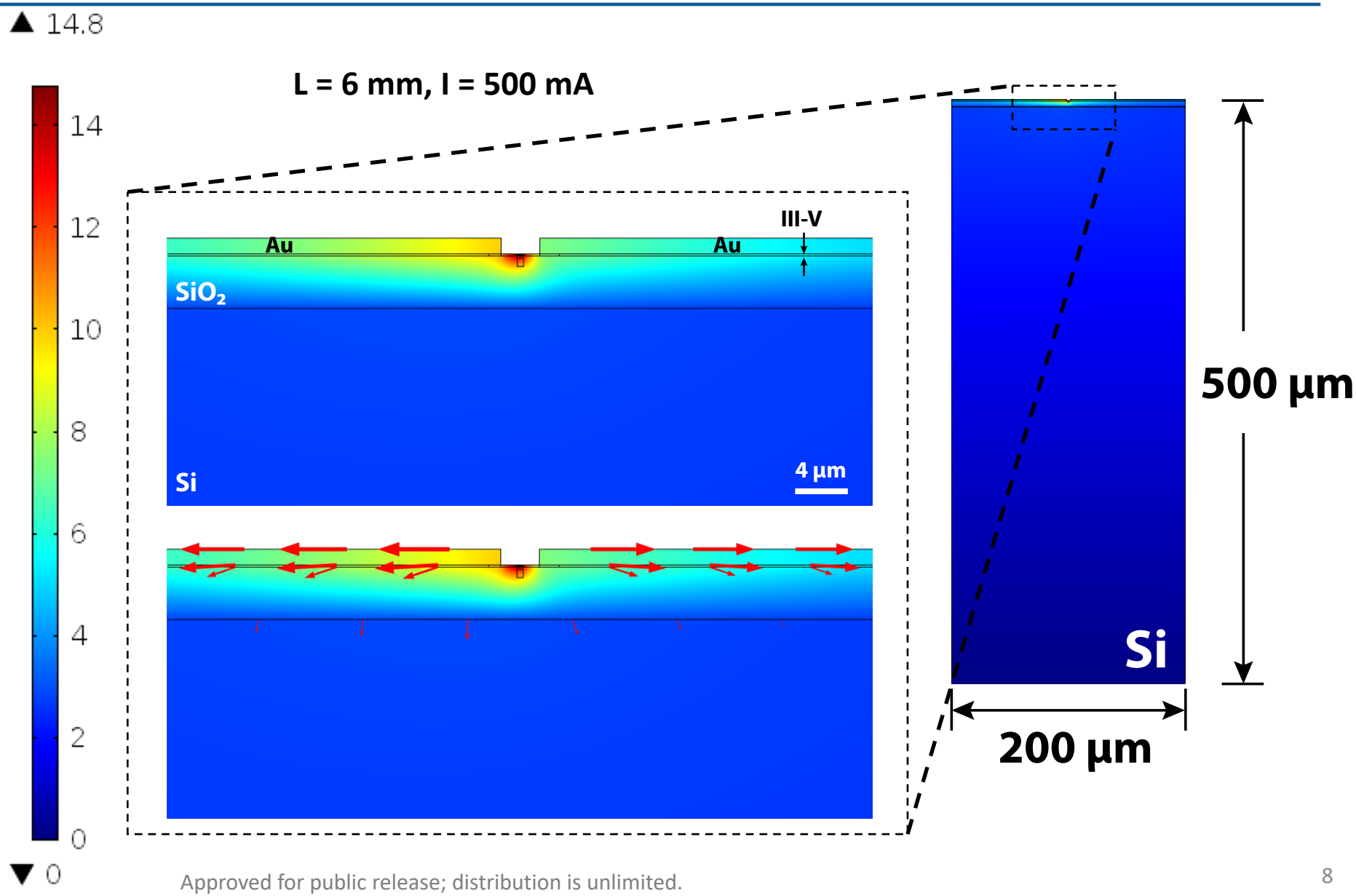

Thermal modeling

Caltech

- Plotted on the right is the temperature rise in the active region as function of the driving current for six different active lengths ($1 - 6\ mm$)
- It is clear that temperature rise drops slows significantly with increasing length, especially for lengths $>\ 2\ mm$

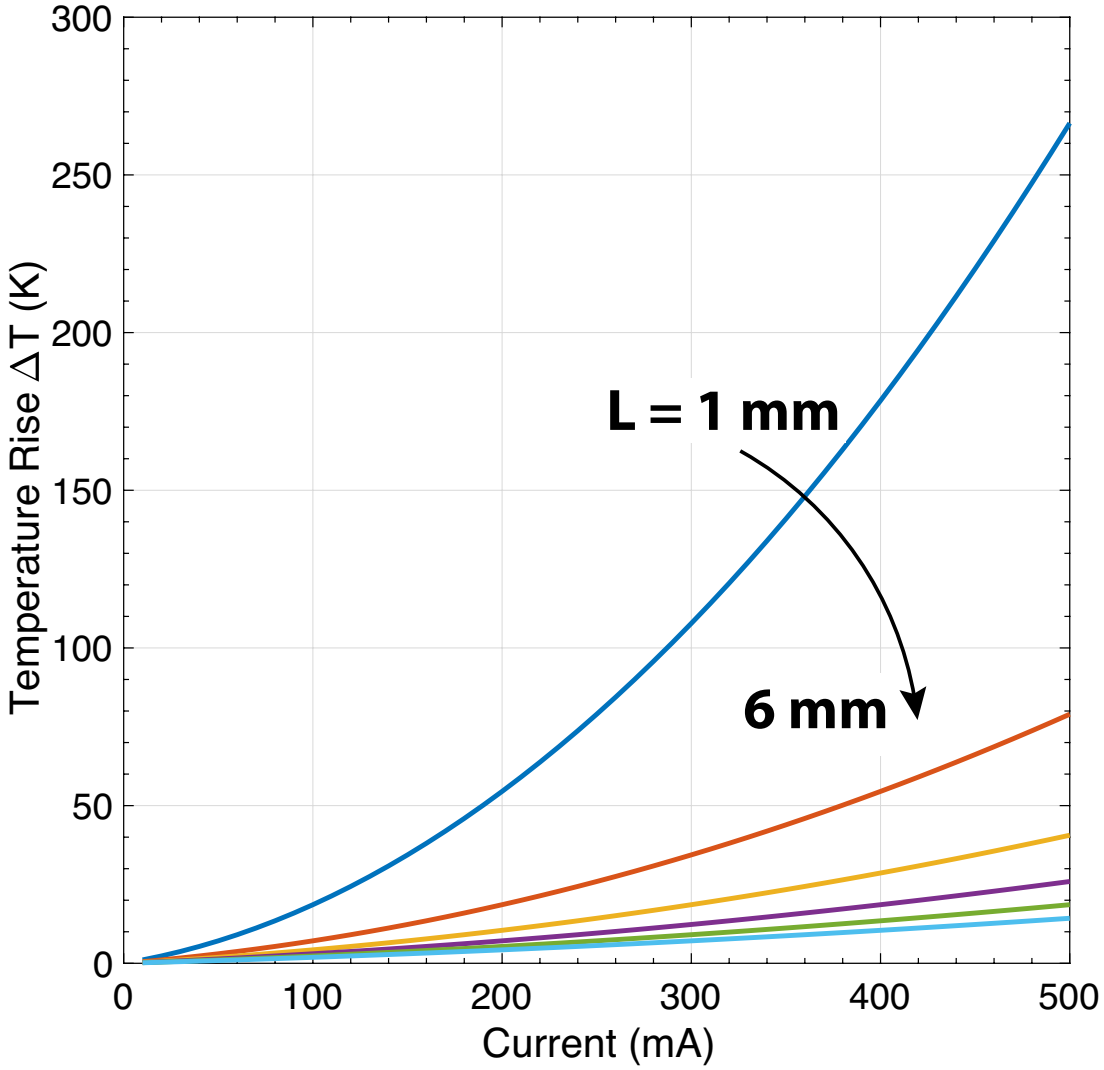

Note: the results of the thermal modeling are based on experimental values for the various resistance components (i.e. series, contact) obtained by MIT-LL

Mode converter

Caltech

- An adiabatic mode converter (AMC) in InP is the critical element responsible for the transfer of optical energy between III-V and SiN
- Simulated snapshots of the various stages of the mode conversion are shown in the figure on the left below
- Near complete (~100%) transfer of energy (not accounting for loss due to scattering) is possible. This is made possible thanks to the reduced thickness III-V thickness ($200\ nm$). As a result, the effective mode index of the InP waveguide can be brought brought close and below, through tapering of its width (W_{tap}), to that of the fundamental SiN waveguide, as shown in the figure on the right below

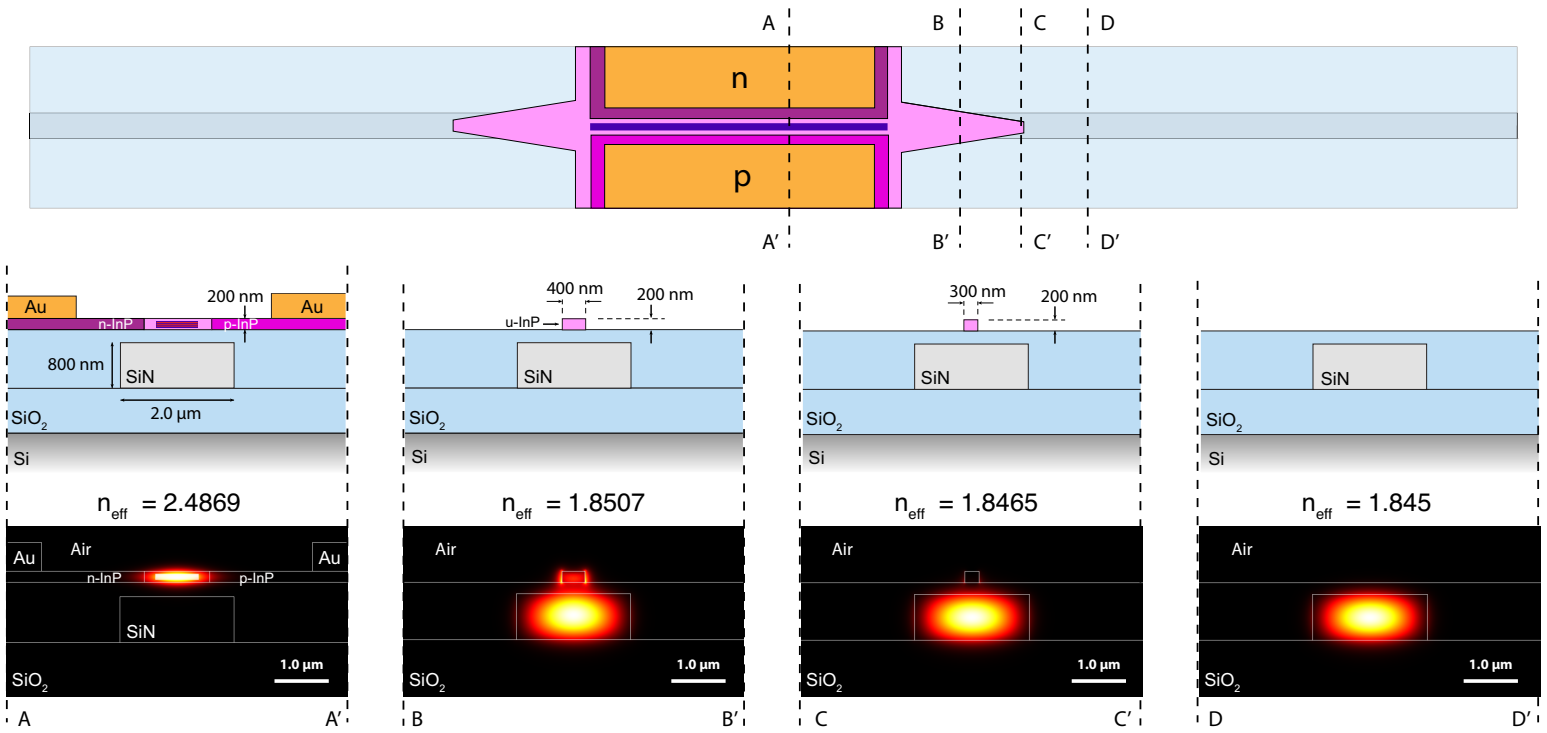

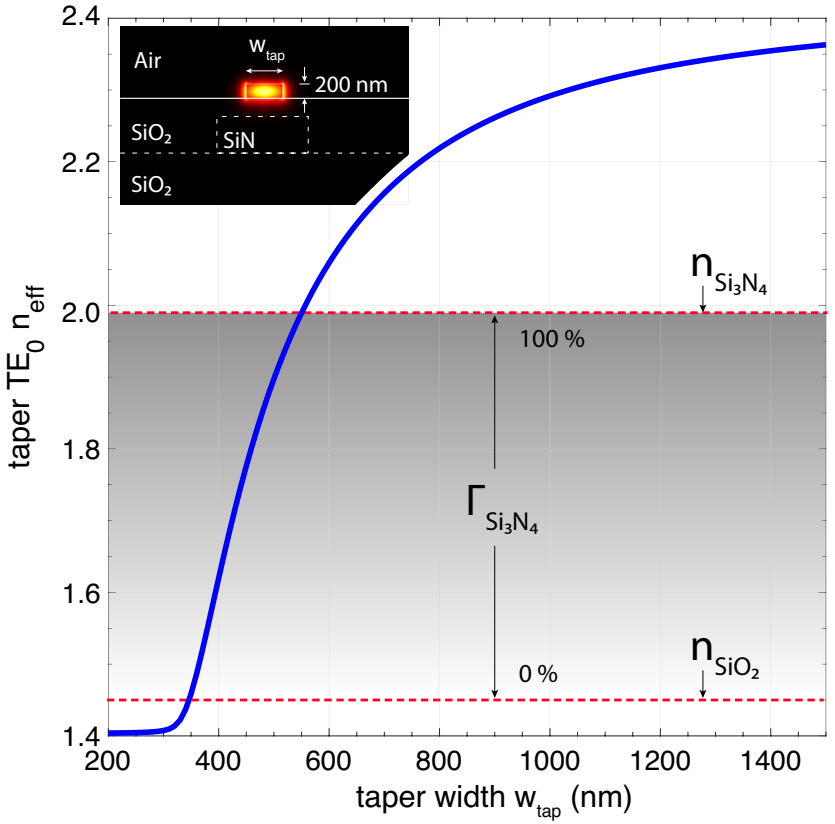

Mode converter

Caltech

- A more detailed description of the AMC design is given in the figure on the right, along will all relevant parameter definitions. The values used for them in the actual, fabricated devices are given in the table on the right below
- The converter comprises 2 stages, a shorter initial one, followed by a much longer 2nd stage. The entire transfer of energy is done over the latter

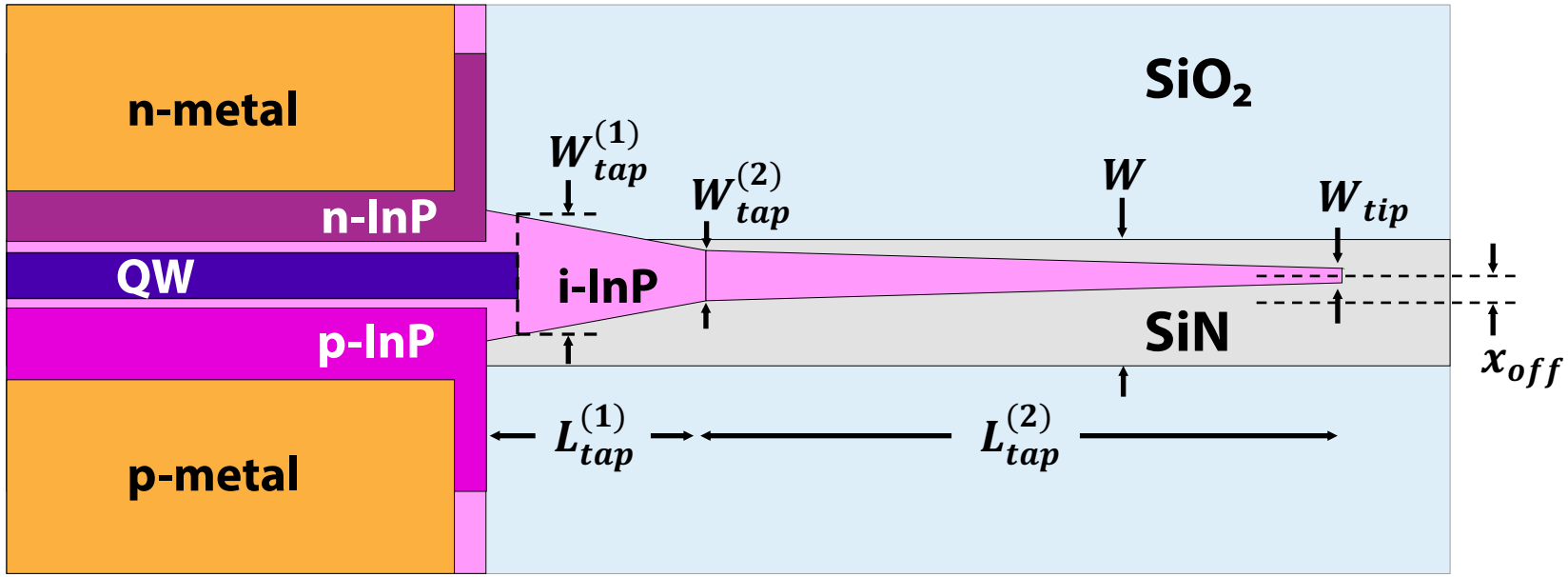

- $L_{tap}^{(1)}$: length of 1st stage
- $L_{tap}^{(2)}$: length of 2nd stage
- $W_{tap}^{(1)}$: starting width of 1st stage (measured from the edge of the QW)
- $W_{tap}^{(2)}$: starting width of 2nd stage
- W_{tip}: taper tip width
- W: width of SiN waveguide over length of taper
- x_{off}: lateral mis-alignment between taper and SiN waveguide

$L_{tap}^{(1)}$	10	μm
$L_{tap}^{(2)}$	100	μm
$W_{tap}^{(1)}$	1.0	μm
$W_{tap}^{(2)}$	0.45	μm
W_{tip}	0.20	μm
W	1.25	μm

Mode converter

Caltech

- An unavoidable imperfection and cause of loss in a real-life mode converter is the lateral misalignment between the InP taper and the underlying SiN waveguide, denoted by x_{off}
- It is important that the AMC is designed so that it can tolerate a realistically expected size of alignment error. In our case that error was $x_{off} < .5\ \mu m$.
- As can be seen in the plot on the right, the AMC is capable of sustaining a total insertion loss $S_{21}^{(2)} < .1\ db$ for errors up to $\sim .45\ \mu m$

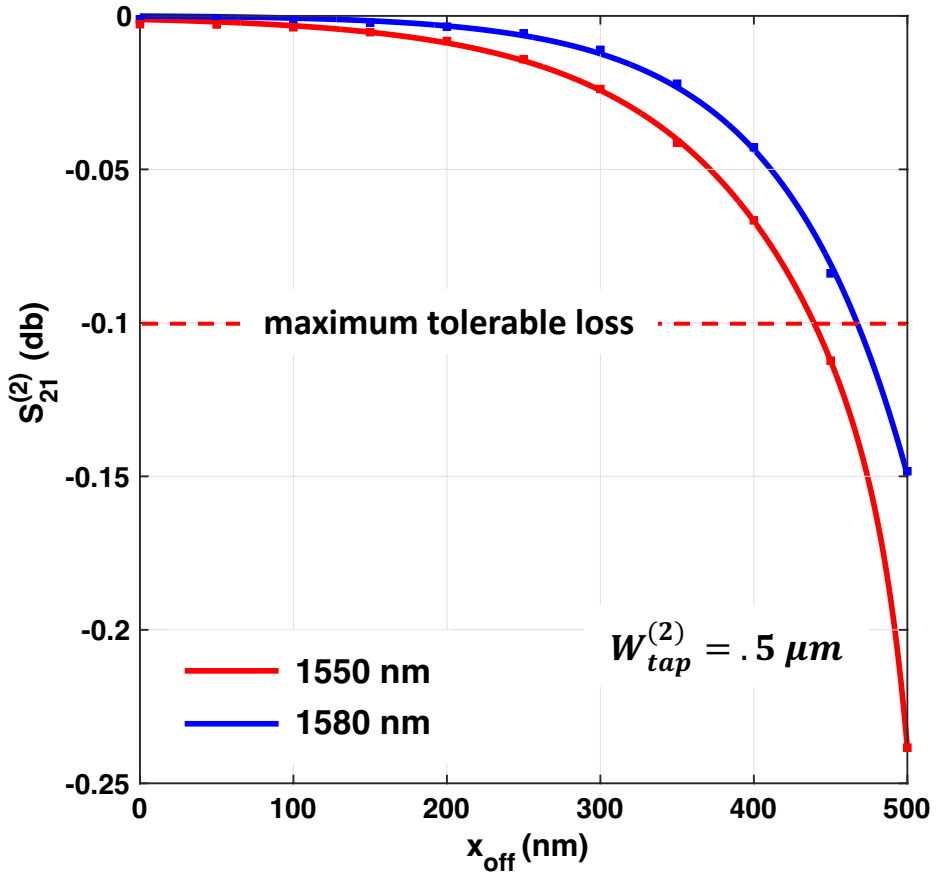

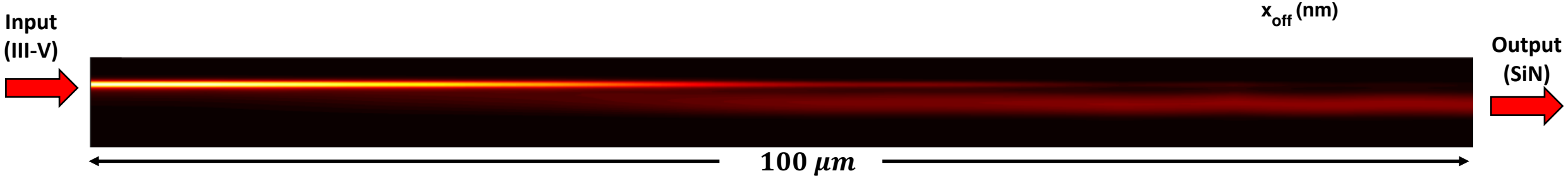

High-Q resonator design

Caltech

- The high-Q resonator is the key determinant of the magnitude of linewidth reduction
- One of the laser's mirrors (see fig. below) doubles as a mirror and a high-Q resonator (i.e. resonant mirror). As such, the resonant mirror's reflection is, in principle, frequency dependent, both its phase and magnitude. The *dispersive* reflection acts as negative feedback to laser phase/frequency fluctuations dependence, thereby, reducing phase/frequency noise and the linewidth associated with it. The higher the Q-factor of the resonator (loaded Q), the larger the magnitude of linewidth reduction

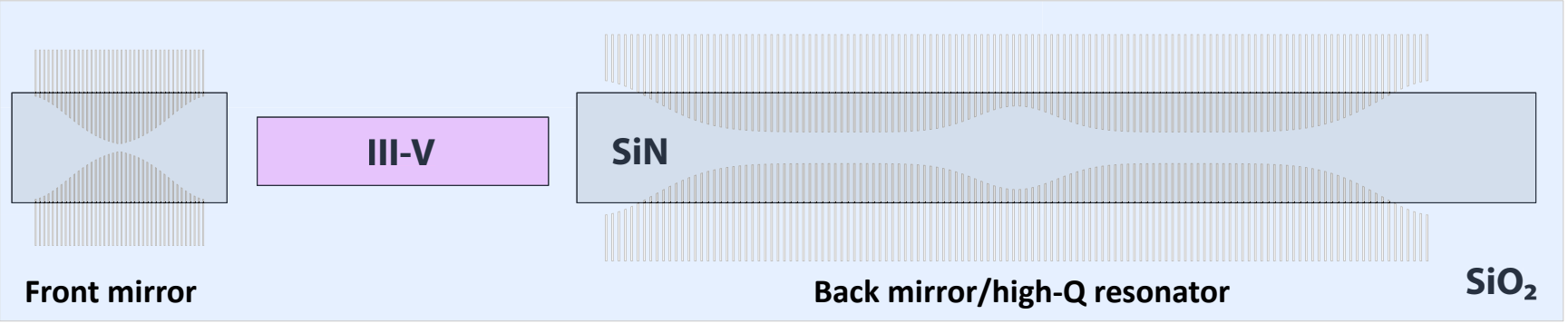

High-Q resonator design

Caltech

- The high-Q resonator is formed through structural modulation of a grating (see top view on the left below). The modulated parameter is the transverse gap between the grooves of the grating, denoted by g_{sp}. The modulation creates a resonant mode inside the grating's stopband (i.e. defect-mode)
- The grating itself is formed by the etching of grooves in the SiO_2 cladding on top of the SiN (see cross-section on the right below). The thickness of the SiO_2 top cladding and, hence, the depth of the grating is $\sim 350\ nm$. Splitting the grating grooves and offsetting them from the center of the waveguide enables access to lower coupling coefficients (κ). This is important for reducing scattering loss and achieving a higher overall Q-factor

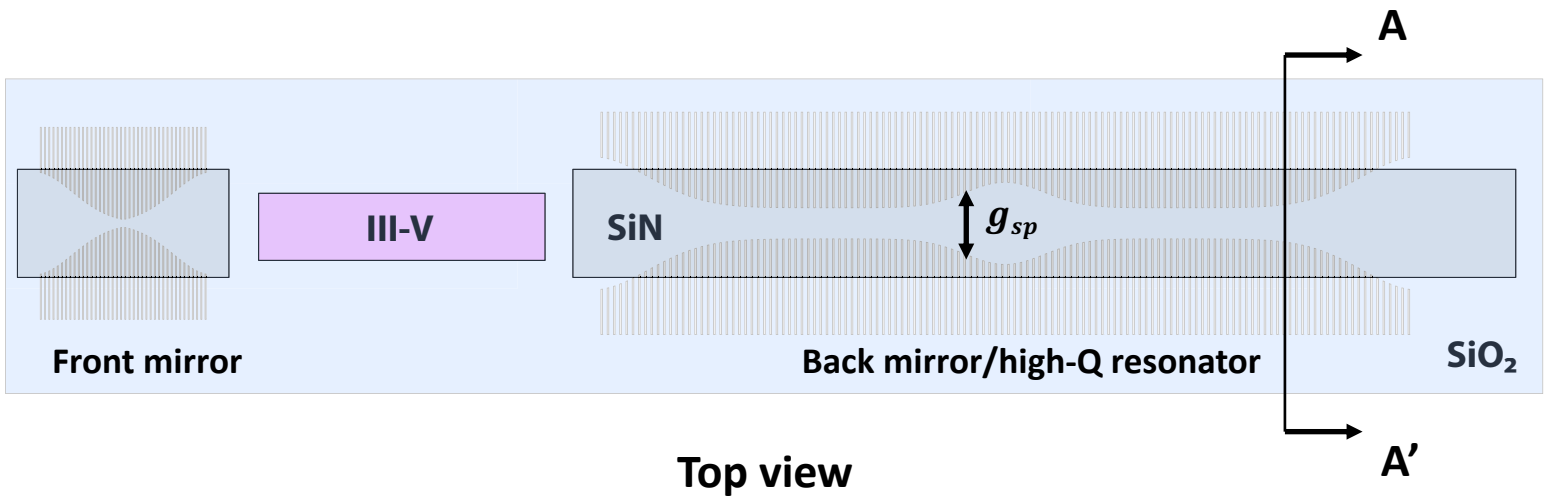

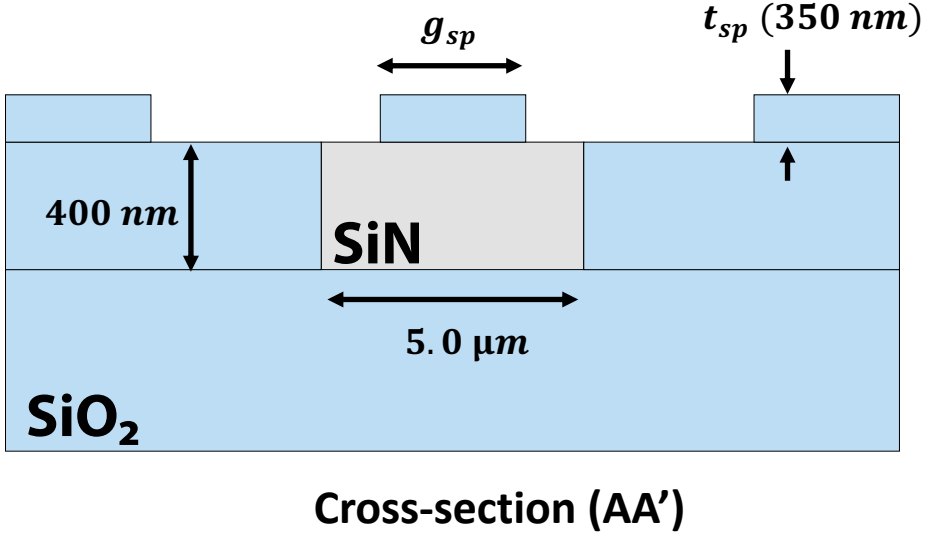

High-Q resonator design

Caltech

- Plotted on the right is the numerically calculated coupling coefficient (κ) as a function of the gap between the grating grooves (g_{sp})
- Lower κ yields less scattering loss, up to the point where scattering is no more the dominating factor, but requires longer grating
- Below is an example of a simulated resonator transmission spectrum. The stopband is indicated by the grey-shaded area (~200 GHz wide), while the high-Q resonance, indicated by the red Lorentzian lineshape, is located ~24 GHz inside of the stopband edge

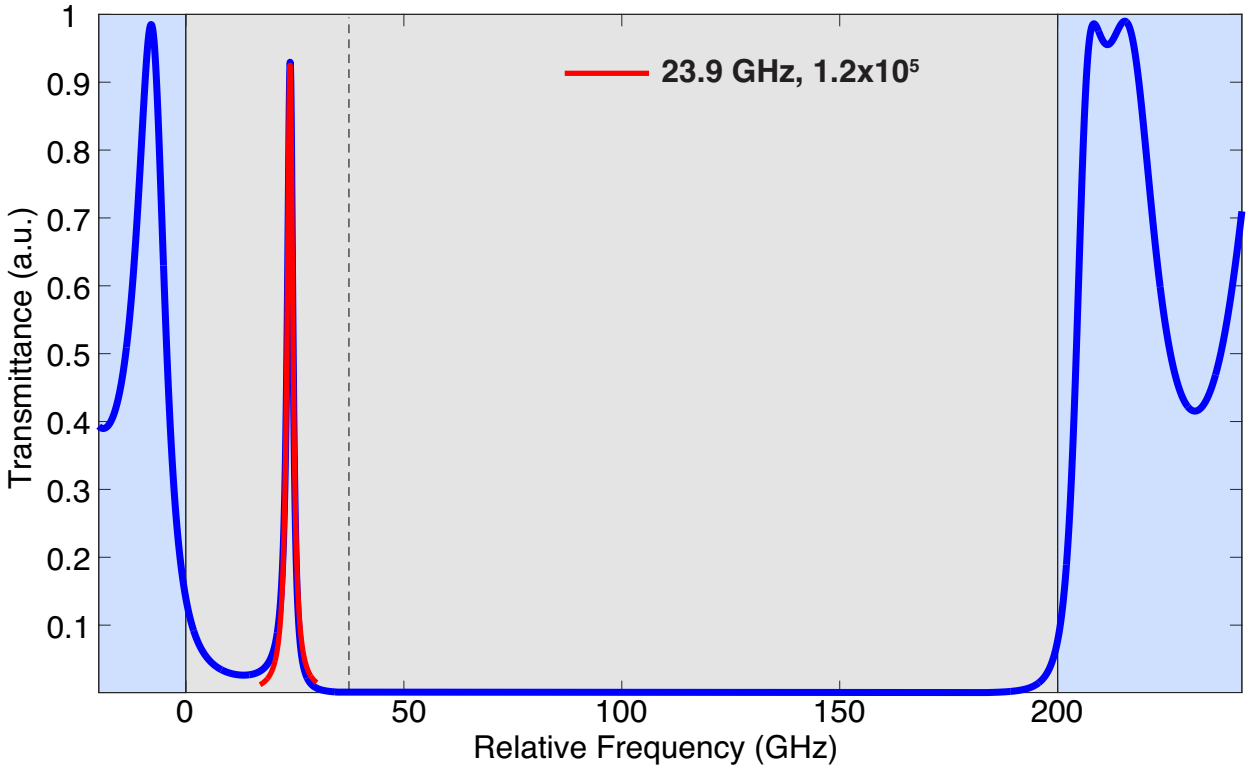

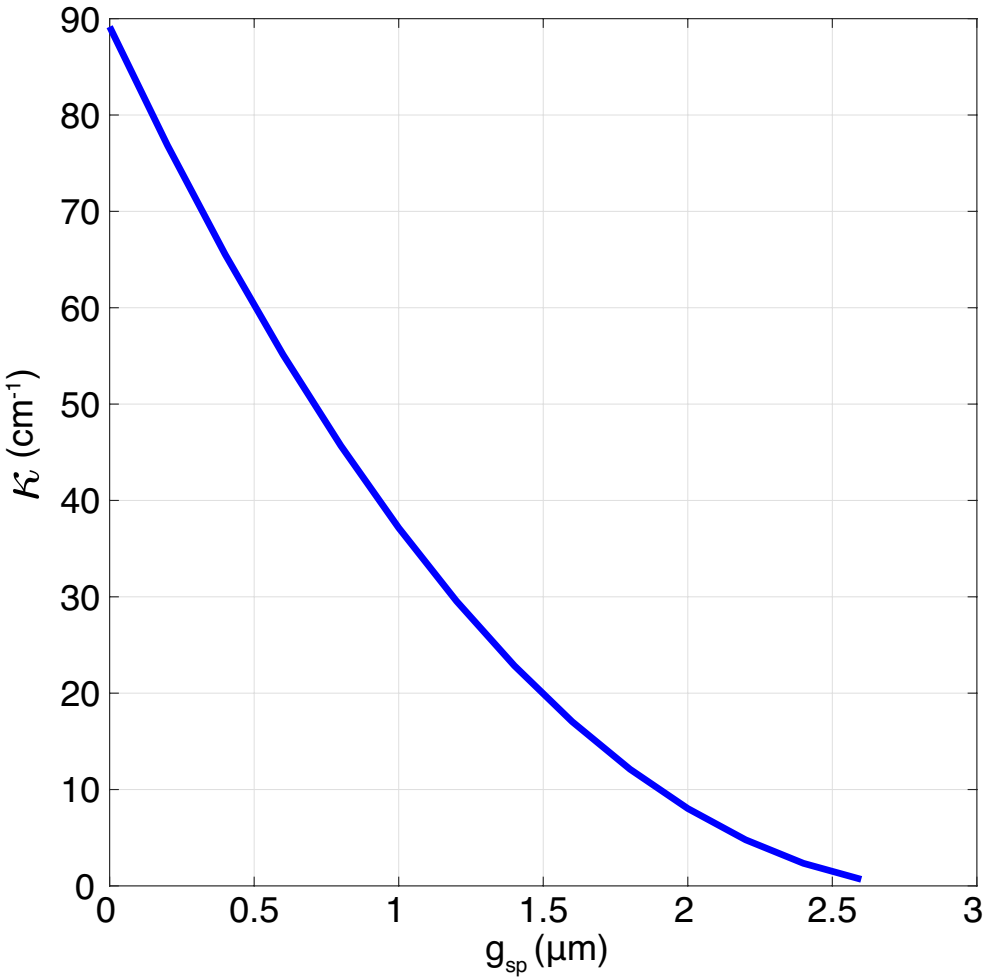

Laser design

Caltech

- **Waveguide design**
  The figure below shows a top-view layout of the SiN waveguide for each laser with all relevant structural definitions

  - Maximum length L_{III-V} is allocated for the III-V (active) section (maximum bondable length). A SiN waveguide need not be present throughout that length, except only on the 2 ends, under the InP AMC
  - Lengths L_{HQ} and L_{mo} are reserved for the high-Q resonator and output mirror grating, respectively
  - The waveguide is bent and flared on both its ends to suppress back-reflection at the facets

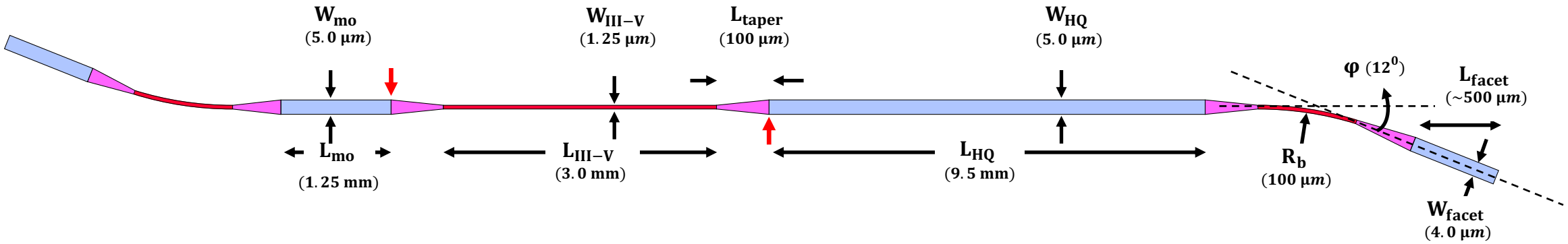

Laser design

Caltech

The specific laser cavity features two distinct types of longitudinal modes

- Modes formed between the two mirror gratings of the Fabry-Perot (F-P) type
- Defect-type mode(s) of the high-Q resonator. In this particular case, the resonator is designed to support only one defect mode

The two types of modes differ significantly in their longitudinal mode profile, examples of each given in the figure on the right. The main differences between the two types of modes are summarized below

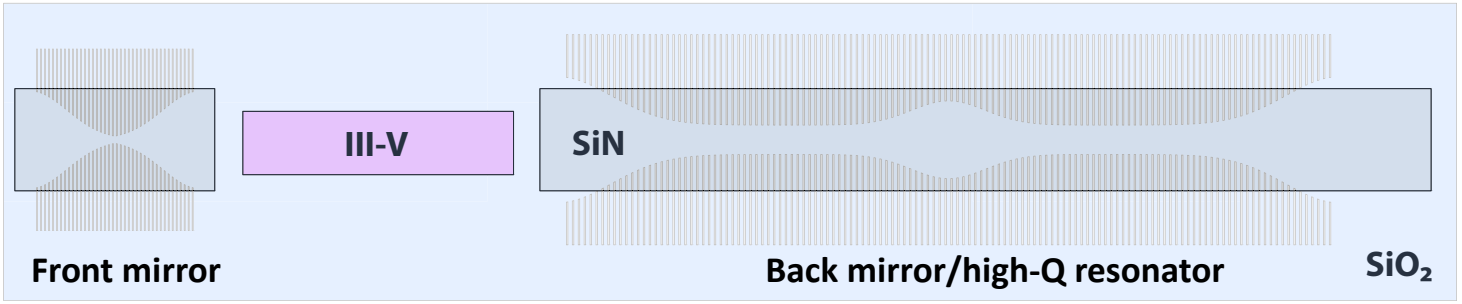

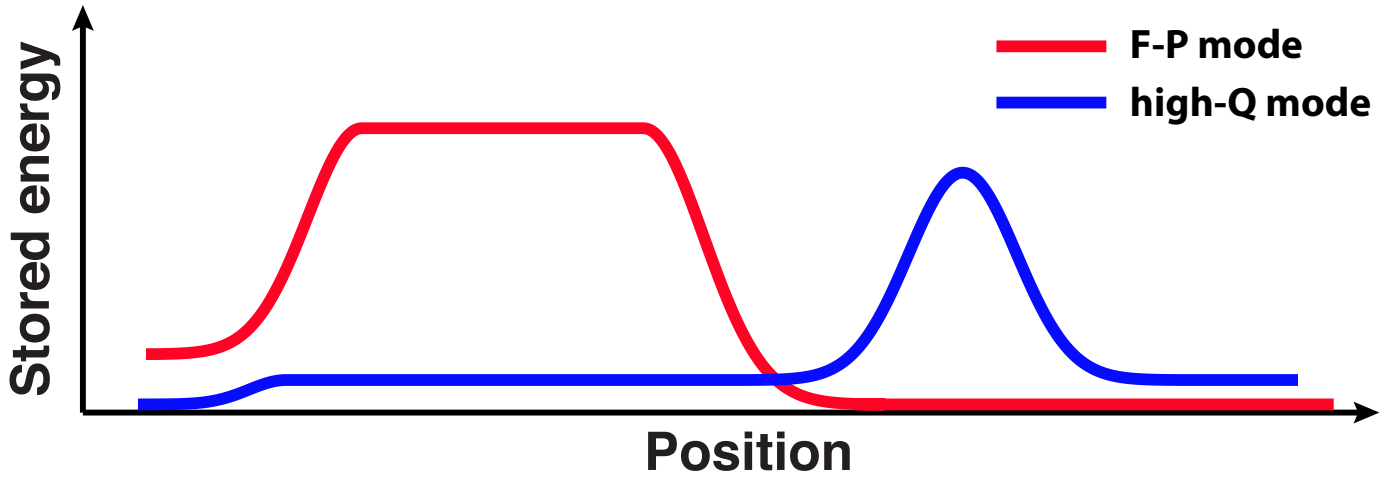

High-Q mode

- Low modal loss / low modal gain
- Non-tunable

F-P modes

- High modal loss / modal gain
- Tunable (e.g. temperature)

Laser design

Caltech

The existence of multitude of modes, both their number and distinct characteristics, pose serious challenge and dilemma for laser design for narrow linewidth

- The challenge lies in the competition between modes for lasing. For narrow linewidth, it is imperative that laser oscillation is maintained single-mode
- F-P modes are more likely to reach lasing first, owing to their overlap with gain (i.e. higher modal gain). However, those same modes (F-P) are unlikely to achieve narrow linewidth, owing to their higher modal loss
- The high-Q mode, on the other hand, is most suited for achieving narrow linewidth, but is unlikely to reach lasing first

We identify two distinct approaches to narrow linewidth:

Approaches to linewidth reduction

1. Low-loss modal energy storage (high-Q mode)
2. Optical feedback (i.e. frequency stabilization) – F-P mode against high-Q mode

Given the considerations above, we deem the 2nd approach as most likely and viable to achieve in the present device configuration

Laser design

Caltech

The approach to linewidth reduction via optical feedback relies on two key design features:

- Intentional mis-alignment between the spectra of the two mirror gratings (red and blue reflection spectra on the right below). This is to create just enough discrimination between the threshold points of the F-P mode set
- Placement of the high-Q resonance close to the stopband's edge ($< FSR$ of the F-P modes)

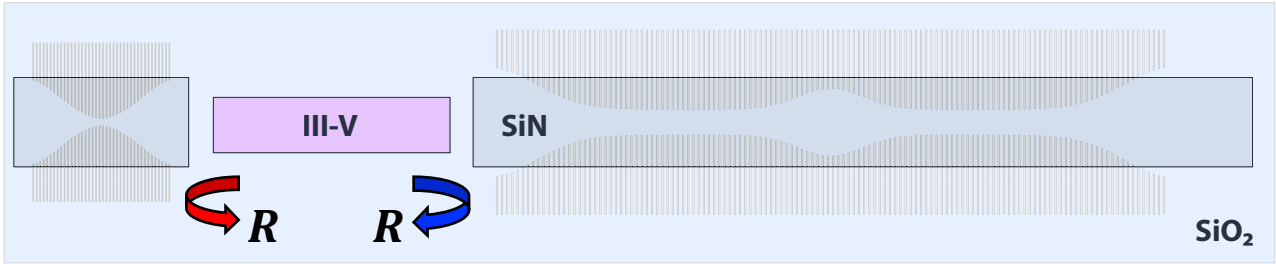

Laser operation is expected to proceed as follows:

1
- F-P modes red-shift (tune to the left in the spectrum on the right) upon current increase due to heating
- Lasing initiated on F-P mode with lowest threshold
- Single-mode oscillation maintained due to gain saturation

2
- Upon further tuning, F-P oscillating mode "lock" to high-Q resonance, triggering linewidth reduction via frequency stabilization

3
- Upon further tuning, "lock" is lost, laser oscillation ceases
- Cycle starts over from 1 (mode-hop)

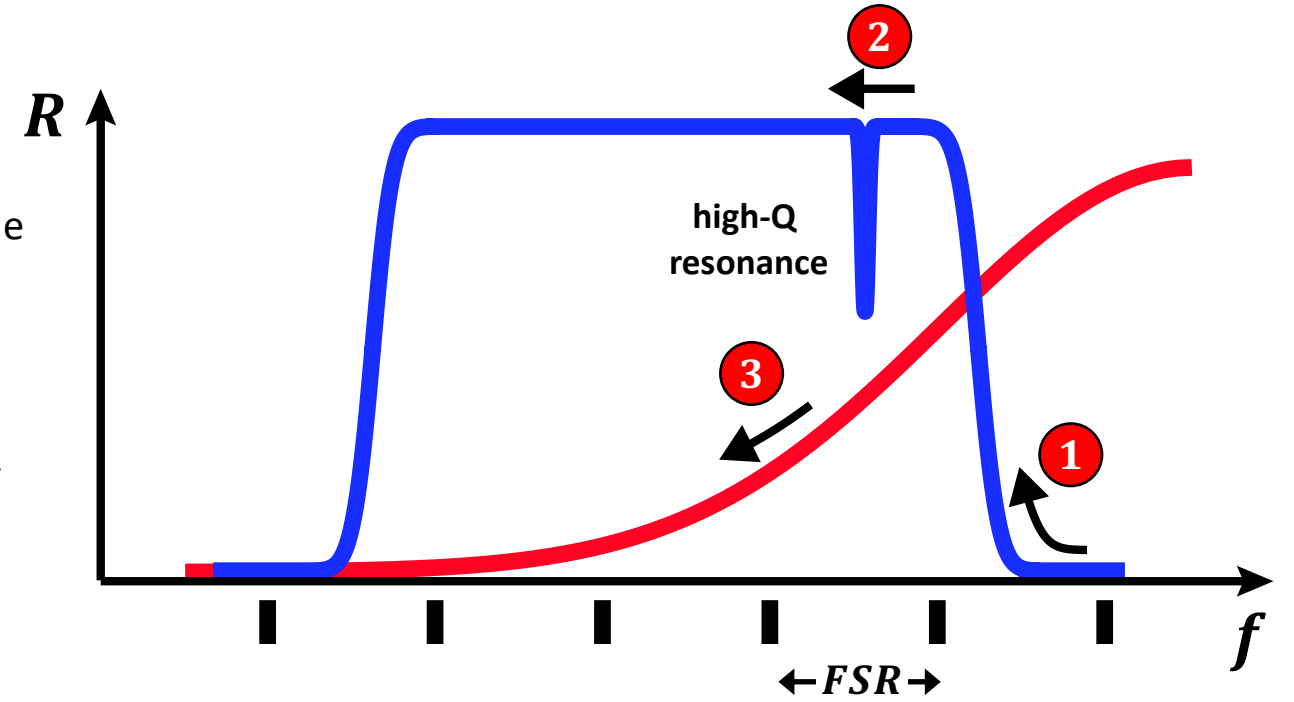

Linewidth reduction

Caltech

Once any one of the F-P modes comes on-resonance with the high-Q mode, its modal loss picks up a strong frequency dependence or, as it's often referred to, becomes *dispersive*. The loss or, equivalently, the photon lifetime (τ_{ph}) can be cast as in equation (1) below, where $\tau_{ph}^{(on)}$, $\tau_{ph}^{(off)}$ are the on-, off –resonance photon lifetimes, respectively. C is a complex constant that depends on the Q-factor of the high-Q resonance and its magnitude is a measure of the magnitude of linewidth reduction

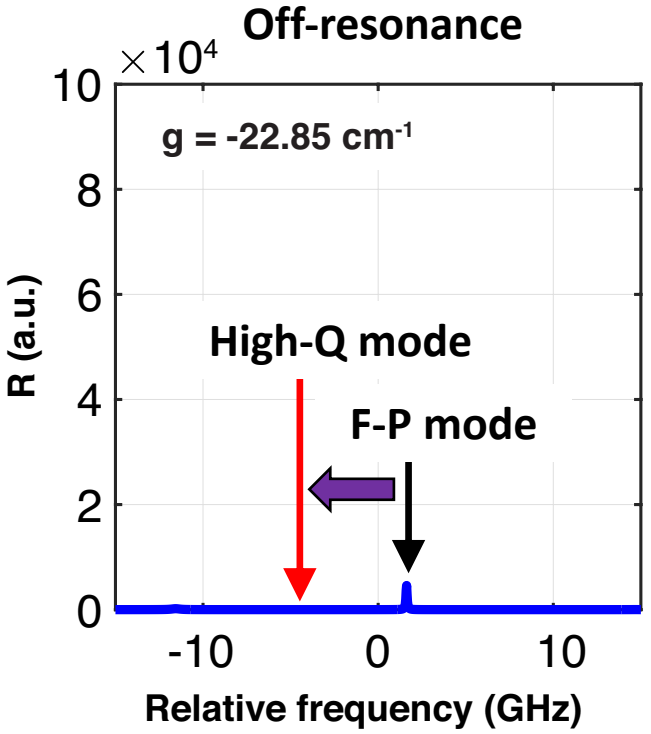

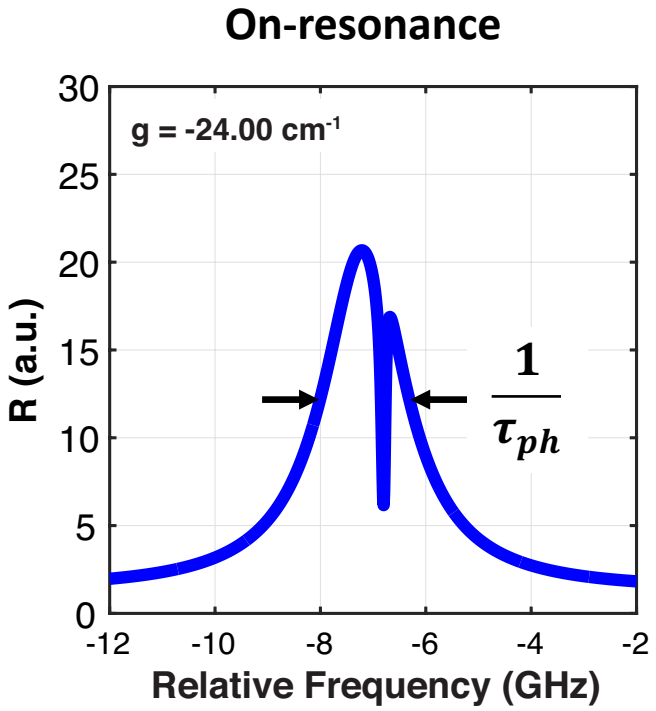

$$\frac{1}{\tau_{ph}^{(on)}} = \frac{1}{\tau_{ph}^{(off)}} + C\dot{\varphi} \qquad (1)$$

- τ_{ph}: F-P coupled-mode photon lifetime (on-resonance)
- $\tau_{ph}^{(o)}$: F-P coupled-mode photon lifetime (off-resonance)
- $\dot{\varphi}$: deviation of instantaneous frequency from central frequency
- C: constant to be determined (in general, complex)

$$S_{\dot{\varphi}}^{(on)} = \frac{S_{\dot{\varphi}}^{(off)}}{(1 + aC_r + C_i)^2} \qquad (2)$$

Frequency noise

Linewidth reduction

Caltech

Shown schematically on the right is the effect of dispersive loss on the laser's frequency noise spectrum ($S_{\dot{\varphi}}(f)$) (red: off-resonance, blue: on-resonance)

- All frequency noise components are reduced by the same amount ($1/C^2$) up to a frequency defined by the bandwidth of the high-Q resonator. Beyond that, the frequency noise reverts back to that of the free-running (i.e. off-resonance) laser
- Optical feedback acts on all types within that bandwidth, regardless of their nature or source (i.e. thermal, quantum, mechanical etc.)
- It is practically "instantaneous" in its response, in that the feedback bandwidth can be fairly wide (~ GHz)

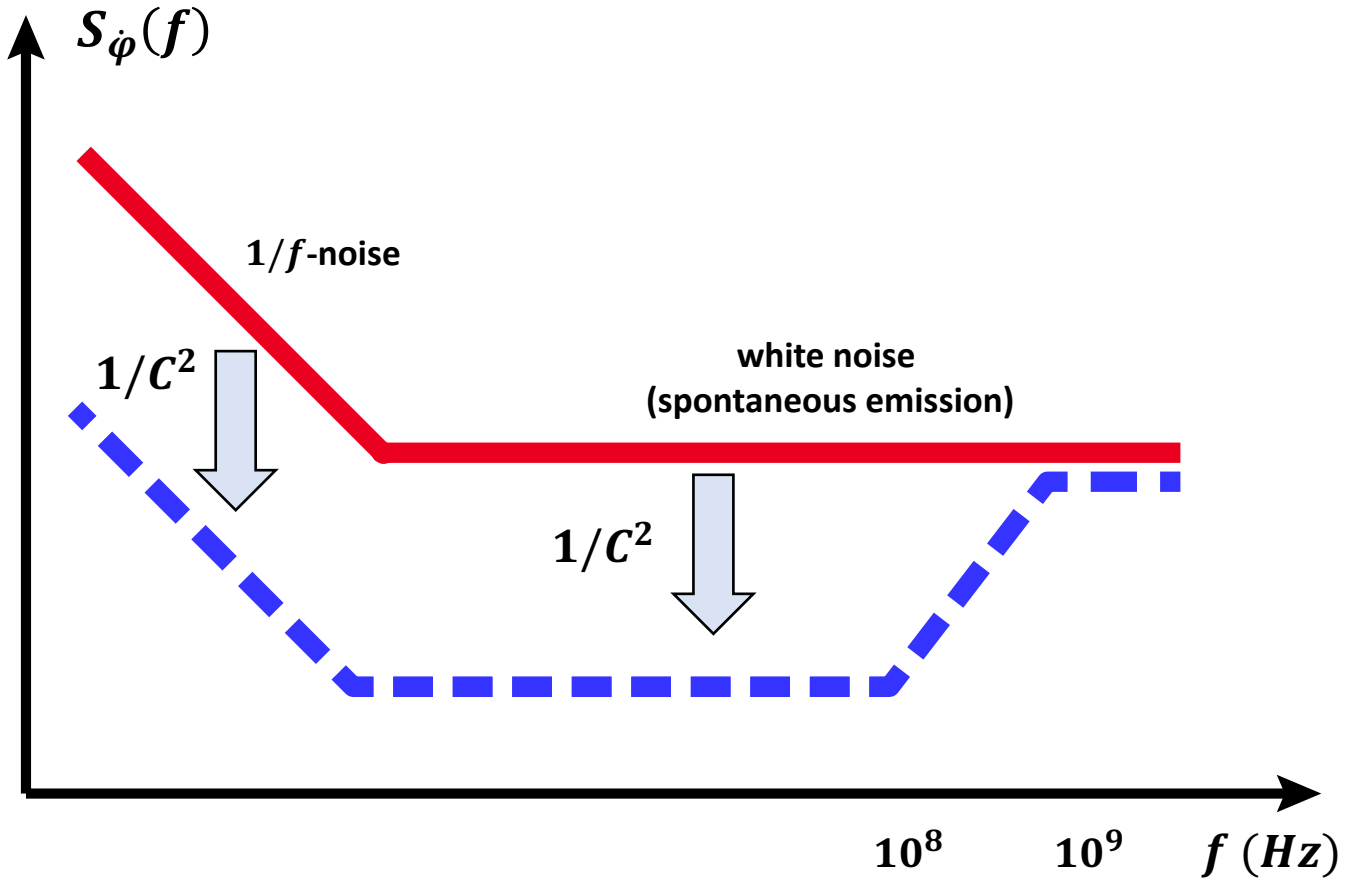

Linewidth reduction

Caltech

Below is a numerical example of the estimation of the expected linewidth reduction for realistic laser and resonator parameters

$$S_{\dot{\varphi}}^{(on)} = \frac{S_{\dot{\varphi}}^{(off)}}{(1 + aC_r + C_i)^2}$$

The laser linewidth due to white frequency noise (i.e. spontaneous emission) is reduced by a factor of C^2, while that due to $1/f$ noise by a factor of C, with respect to their respective off-resonance values

$$C = 1 + \sqrt{\eta(1 + a^2)}\frac{Q_{SiN}}{Q_o}$$

Numerical example:

$a_i + a_m = 40\ cm^{-1} \longrightarrow Q_o \simeq 2.5x10^3$

$a_{SiN} = .1\ db/cm \longrightarrow Q_{SiN} \approx 2x10^6$

$\eta = 1 - R \approx .5$

$a \approx 3$

$C \approx 1.8x10^3$

$C^2 \approx 3.2x10^6$

	$\Delta\nu_{w.n.}$	$\Delta\nu_{1/f}$
off-resonance	30 MHz	3 MHz
on-resonance	10 Hz	2 kHz

white noise linewidth $\Delta\nu_{w.n.}^{(on)} = \frac{\Delta\nu_{w.n.}^{(off)}}{C^2}$

$1/f$ linewidth $\Delta\nu_{1/f}^{(on)} = \frac{\Delta\nu_{1/f}^{(off)}}{C}$

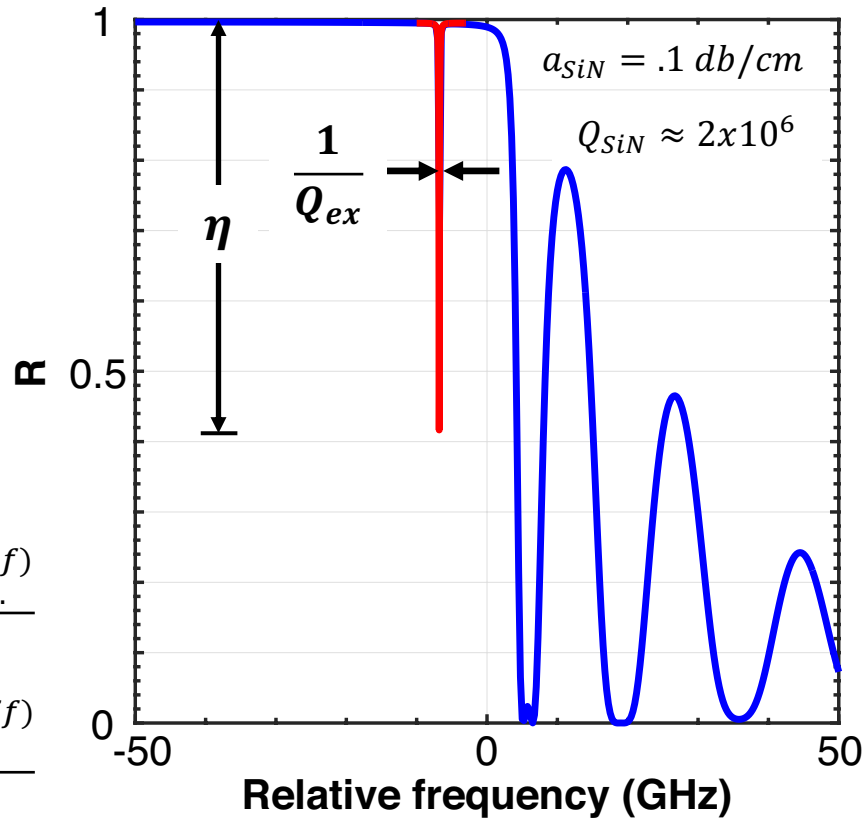

EXPERIMENTAL RESULTS

High-Q resonator characterization

Caltech

- Key input parameter to the final laser design is the intrinsic loss of the high-Q resonator, quantified by its intrinsic Q-factor, Q_i
- We designed sets of high-Q resonators for the MIT-LL SiN platform ($400\ nm$ thickness), according to the designs principles laid out before and the schematic below
- The experimentally measured Q (i.e. linewidth) of any given resonator is known as the loaded Q, expressed as:

$$\frac{1}{Q_L} = \frac{1}{Q_i} + \frac{1}{Q_{m1}} + \frac{1}{Q_{m2}}$$

, where Q_{m1}, Q_{m2} are Q-factors associated with loss (coupling loss) to the waveguide through each of both mirror ends. Varying (i.e. increasing) either or both of Q_m, for example, by varying the length of the respective mirror grating, and measuring Q_L, we expect to obtain a trend like the one in the figure on the right below. The "saturating" value of Q_L corresponds to the resonator's Q_i. This is predicated on the assumption that Q_i remains constant between resonators

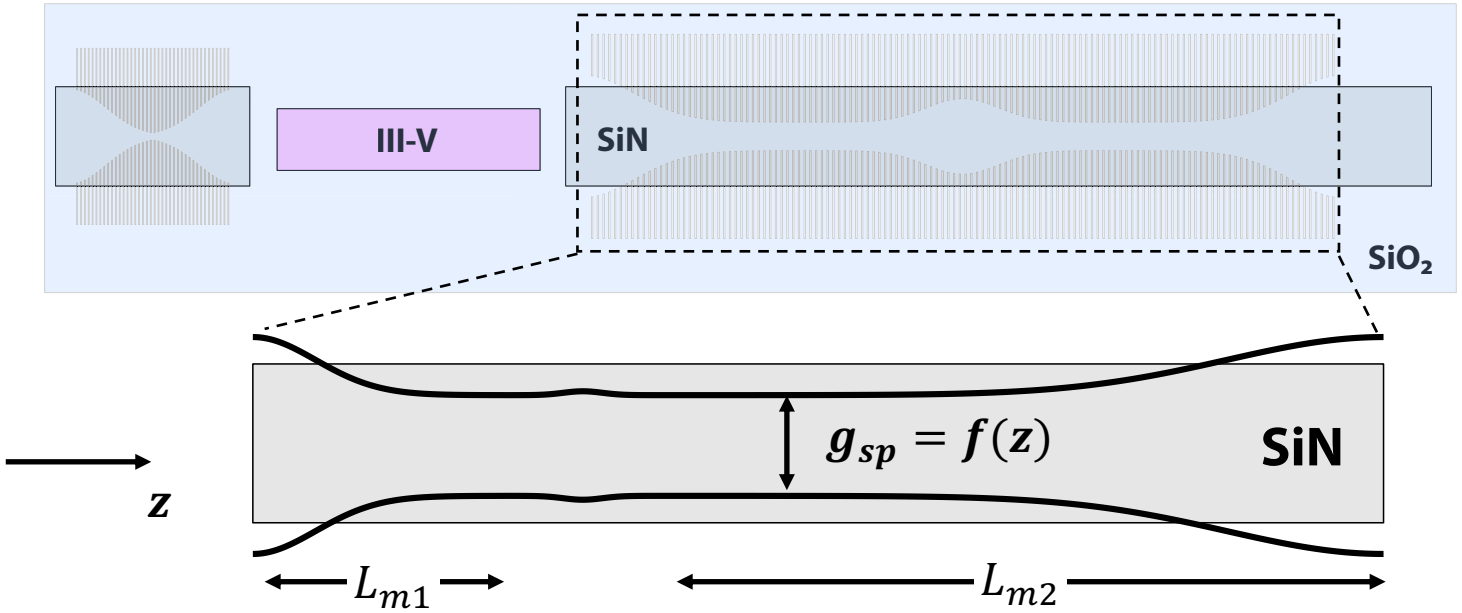

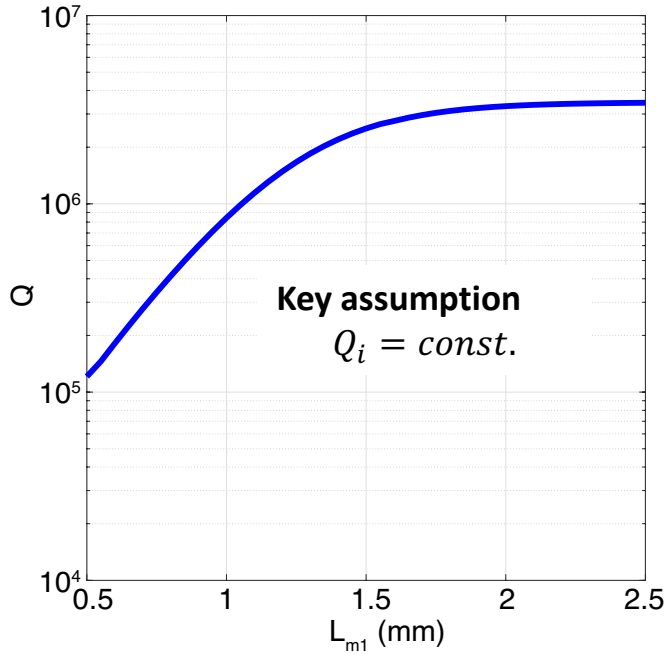

High-Q resonator characterization

Caltech

- Unfortunately, there was no clear Q_L vs Q_m trend established through measurements. This is, most likely, due to Q_i varying too much between resonators. This is also reflected in the normalized transmission not varying monotonically (e.g. decreasing) with Q_m (e.g. increasing)
- On the right is an example of a measured resonator transmission spectrum (normalized transmission). The resonance of interest is that indicated by the red Lorentzian lineshape fit. The linewidth of the resonance yields Q_L
- Absent a clear, saturating for Q_L, an alternate way of estimating Q_i is by using the measured normalized transmission

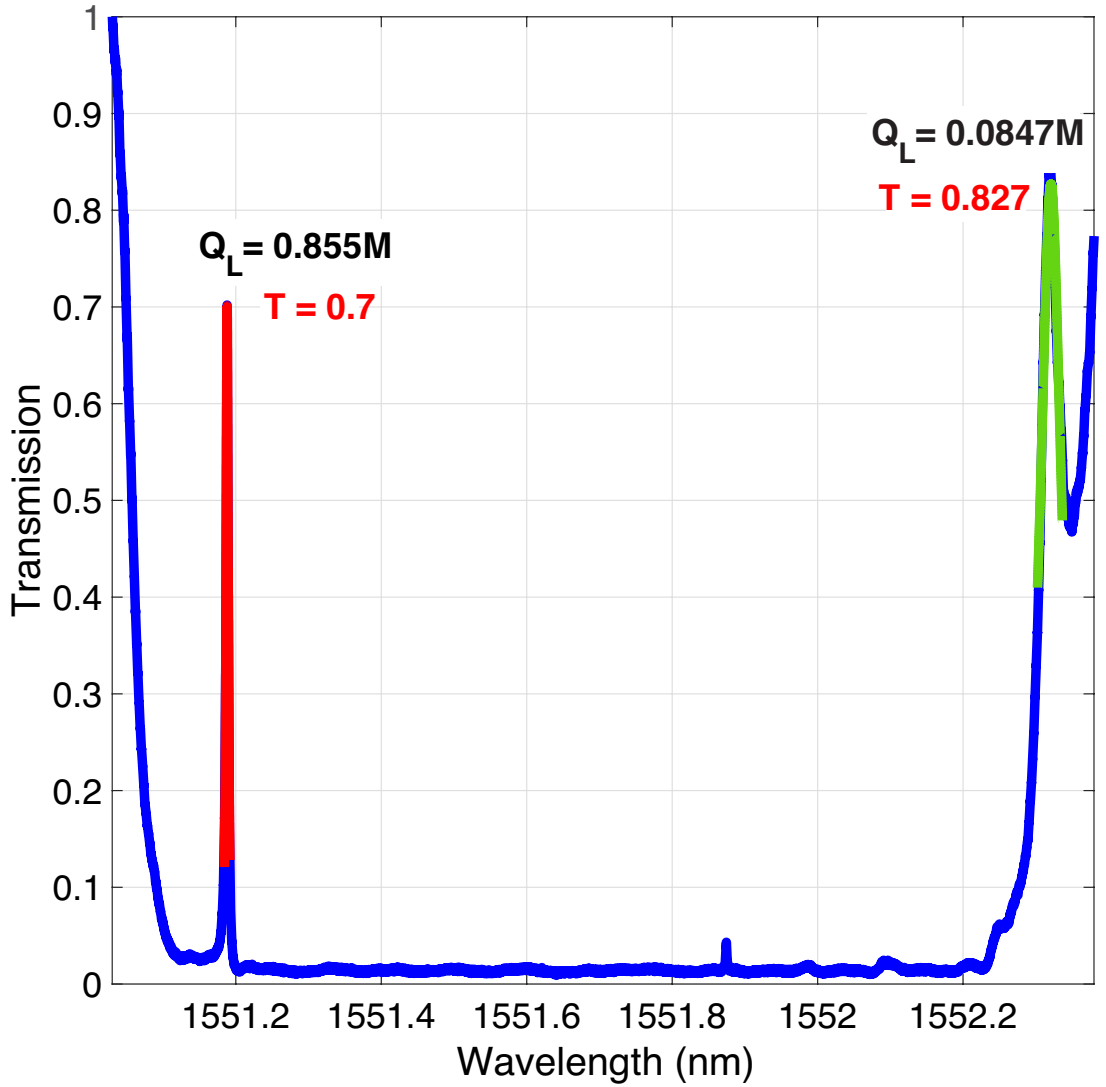

High-Q resonator characterization

Caltech

From coupled-mode theory (CMT), the normalized transmission through the resonator can be expressed as:

$$T = \frac{4Q_L^2}{Q_{m1}Q_{m2}} \qquad (1)$$

By design, $\frac{Q_{m2}}{Q_{m1}} \equiv x > 1$ (2)

Combining (1) and (2) and substituting into:

$$\frac{1}{Q_L} = \frac{1}{Q_i} + \frac{1}{Q_{m1}} + \frac{1}{Q_{m2}} \qquad (3)$$

allows us to solve for Q_i as a function of T and with

$$Q_i(x) = \frac{Q_L}{1 - \frac{x+1}{\sqrt{x}}\frac{\sqrt{T}}{2}} \qquad (4)$$

High-Q resonator characterization

Caltech

- Plotted on the right is $Q_i(x)$ for 4 different resonators
- By design, we know that $x \to 1$, though there is some degree of uncertainty due to imperfect translation from design to reality through fabrication. This uncertainty is represented by the grey-shaded area
- For $x \to 1$, we can extract a estimate range for Q_i , $Q_i \sim 2 - 7M$
- In other words, 2M is a lower bound on Q_i, with a significant degree of variability
- If true, >2M satisfies the requirement set for Q_i

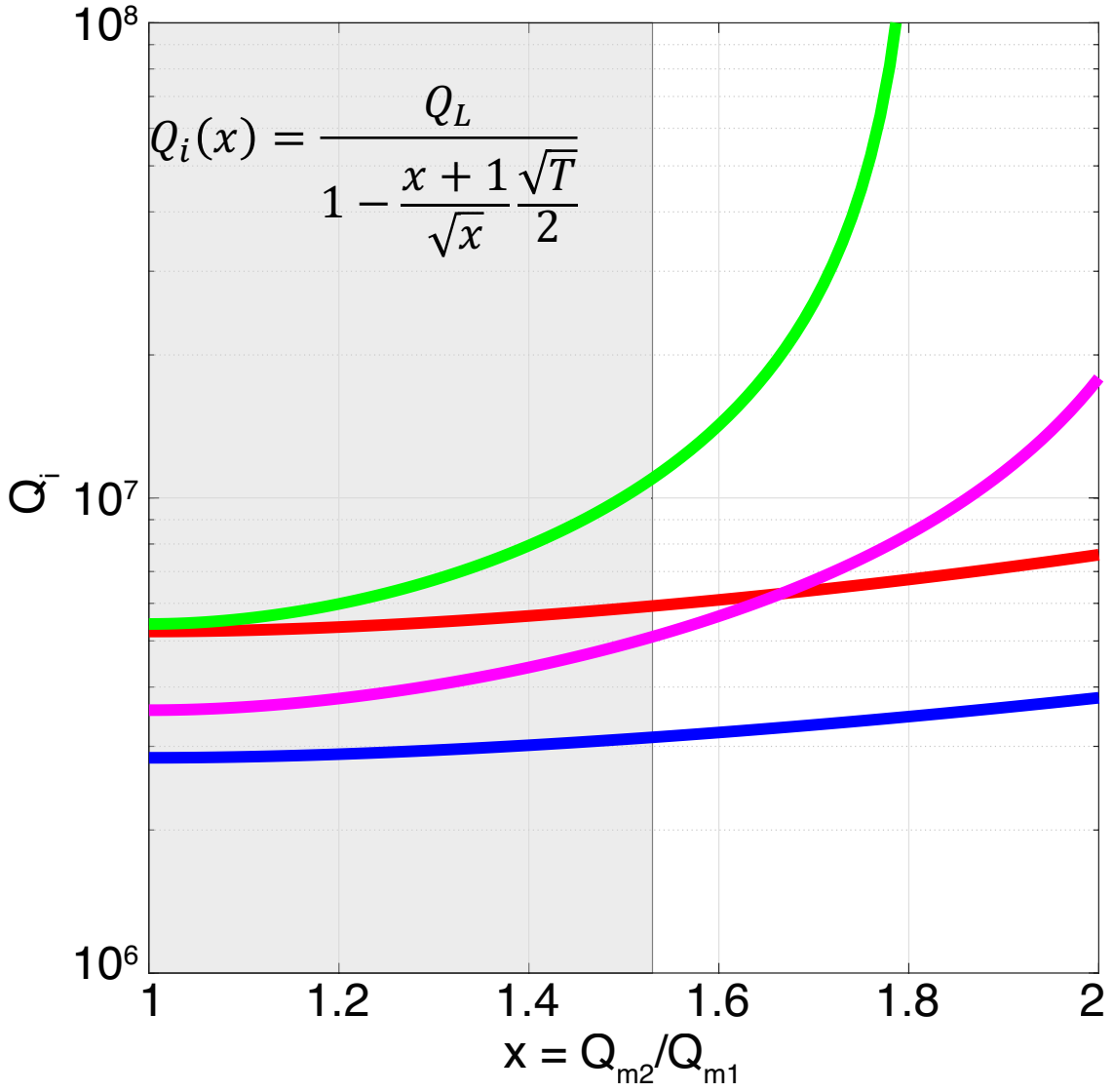

High-Q resonator characterization

Caltech

- Another key feature of the laser design, as mentioned earlier, is the intentional misalignment between the spectra of the its two mirrors. We performed a check of the ability and accuracy of producing the desired alignment in a real device. Below is an example of a side-by-side comparison between design and experiment
- Red and blue traces represent transmission spectra through front mirror (output) and back mirror (high-Q resonator), respectively. There is a fairly close agreement between design and experiment, with a recorded translation error of $\sim .5\ nm$, which is to be taken into account in the laser design

Theory

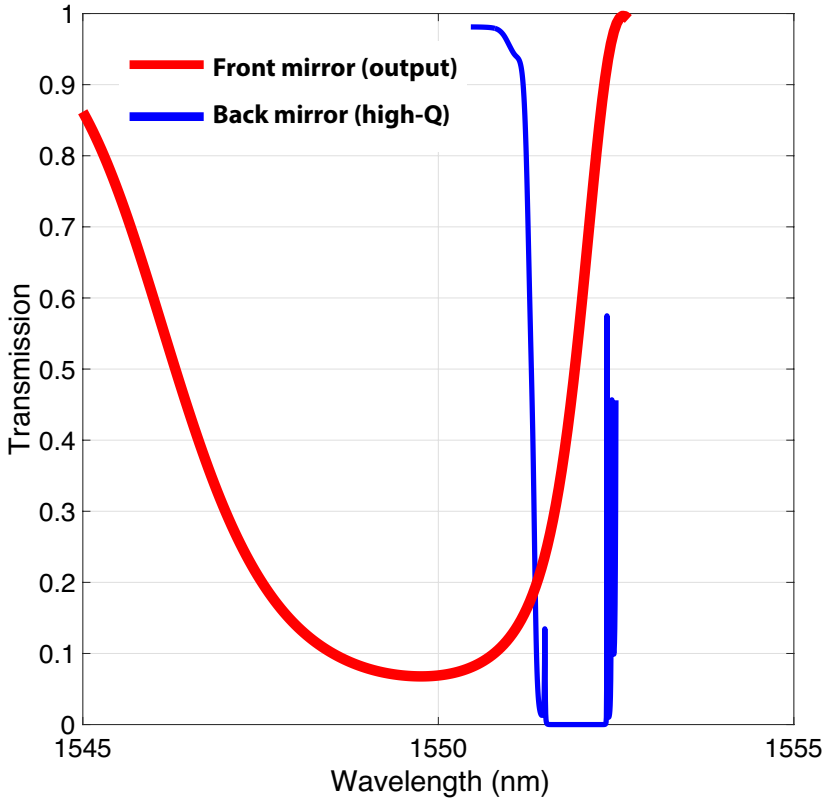

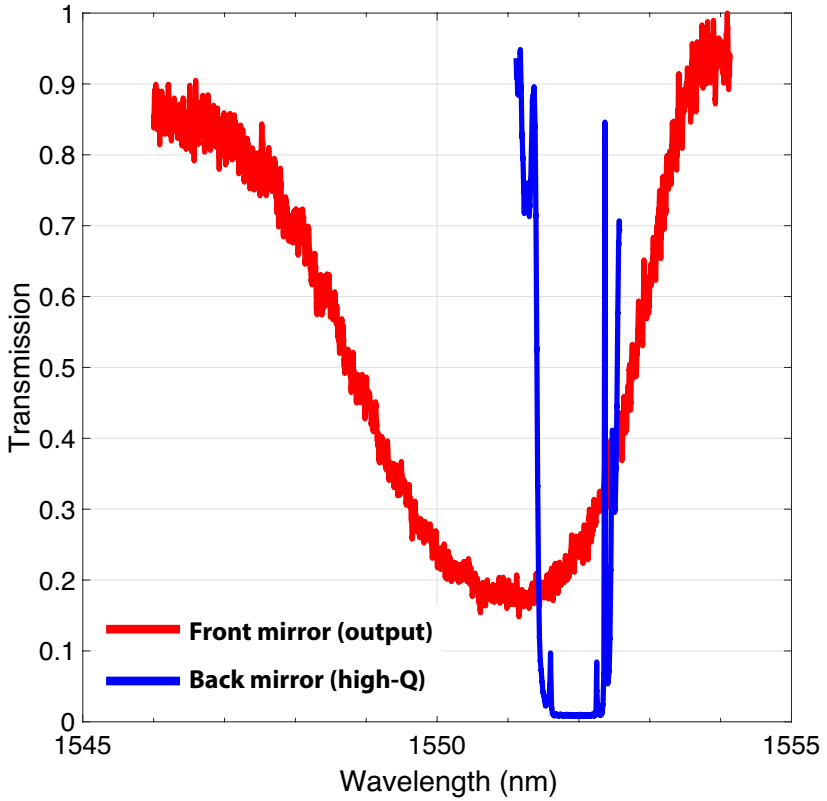

Experiment

Laser characterization

Caltech

- Following the completion of the fabrication of the lasers, MIT-LL performed a preliminary characterization
- That characterization showed no evidence of working devices, as in lasers oscillating continuous-wave (CW) at room temperature
- Upon receiving the lasers at Caltech, we focused on collecting more data in search of clues as to the failure of the devices to operate as intended

Laser characterization

Caltech

- The first set of measurements was light output power as a function of drive current (L-I). Below are two representative examples
- As already suspected, there is no evidence of lasing RT-CW
- Additionally, an early (~ 100 mA) onset of power saturation and subsequent roll-off indicates possible overheating

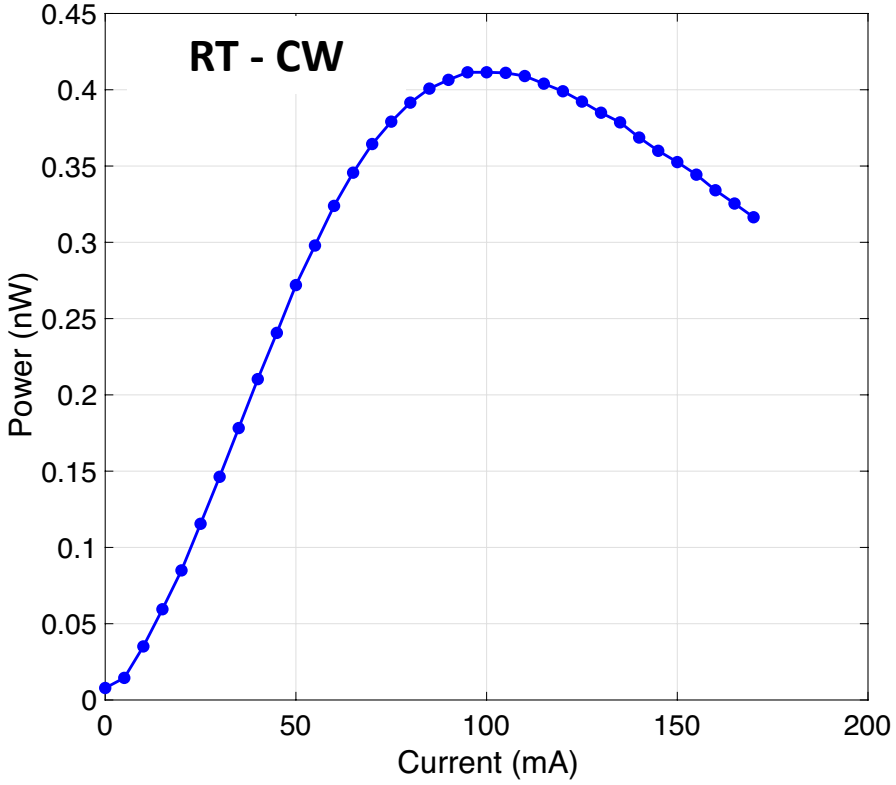

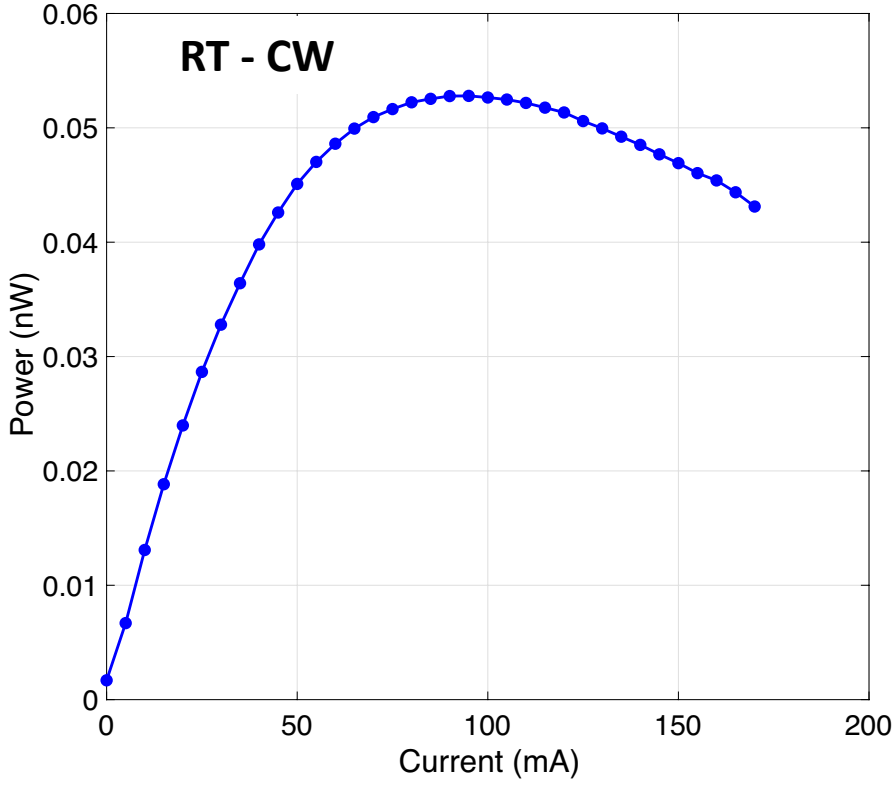

Laser characterization

Caltech

- On the right is another example of a L-I measurement, along with a I-V measurement taken by MIT-LL
- From the I-V characteristic, we extract an experimental differential resistance (i.e. series resistance) of $\sim 25\ \Omega$
- This is about 2.5x higher than the expected resistance of $\sim 10\ \Omega$ for the specific active length (1.5 mm), based on prior resistance characterization (TLM measurements)
- A possible explanation for the higher resistance, as speculated by MIT-LL, is an issue with doping
- This miss in resistance is further proof of resistive overheating as a dominant issue with these devices

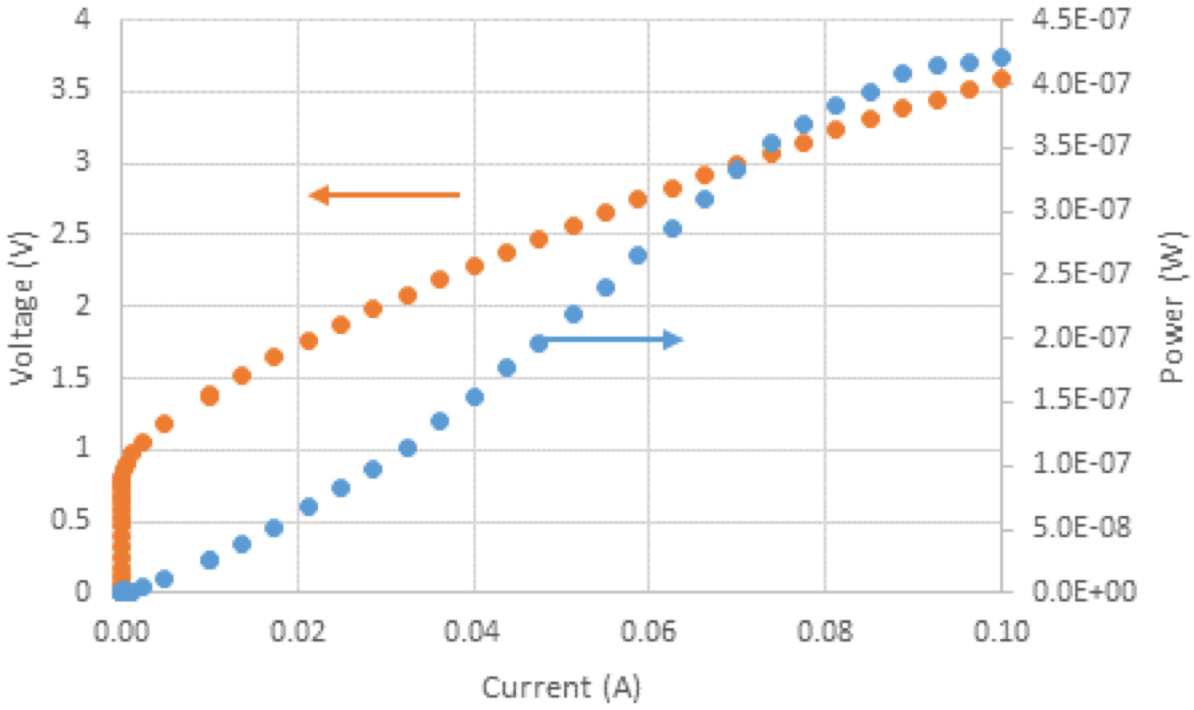

Source: MIT-LL

Laser characterization

Caltech

- The second set of measurements we conducted was that of the optical spectrum of the output light from these devices
- Below are two examples of such measurements. For comparison, on the left is an example of an optical spectrum taken by Caltech and on the right one by MIT-LL
- In both cases, the peak of the amplified spontaneous emission spectrum (ASE) is found to be around $1580\ nm$
- Also discernible on the spectra are signatures of the first two in order (TE_0, TE_1) stopbands of the lasers' gratings. Their spectral locations are indicated by red arrows and are consistent with their respective locations previously determined during the high-Q resonator characterization
- The fundamental stopband (TE_0) is found to be $\sim 30\ nm$ away off the ASE peak (i.e. gain peak), suggesting significantly reduced available gain at the wavelength where the laser is designed to operate (~1550 nm)

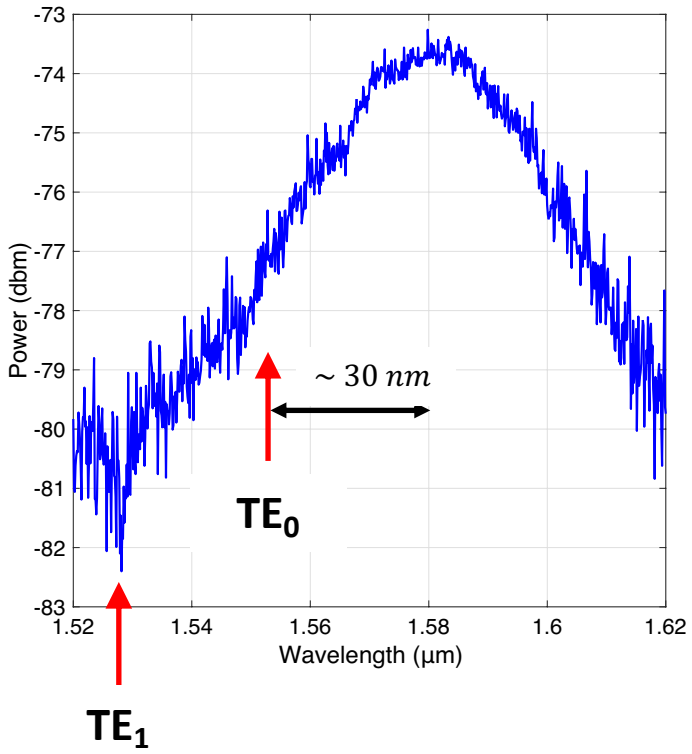

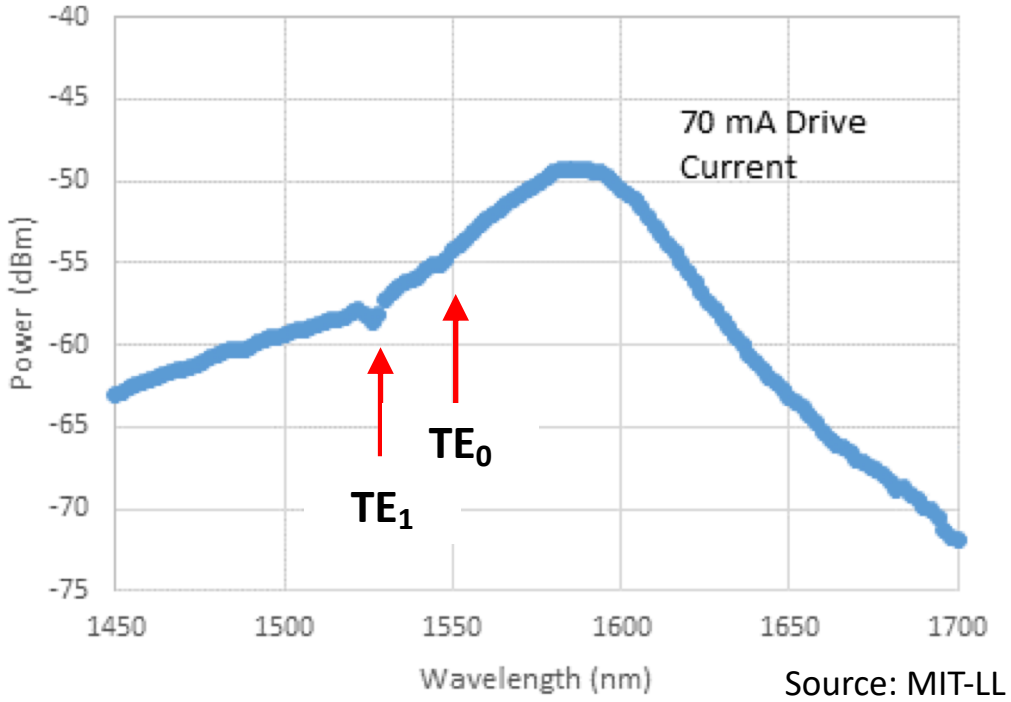

Source: MIT-LL

Laser characterization

Caltech

- To further confirm overheating as one of the culprits for lack of lasing, we performed L-I measurements with pulsed drive
- Below is an example of a L-I measurement with continuous drive (on the left) and one with pulsed drive (on the right) for the same device
- The pulsed L-I exhibits a familiar kink, albeit somewhat smooth, indicative of laser threshold

CW

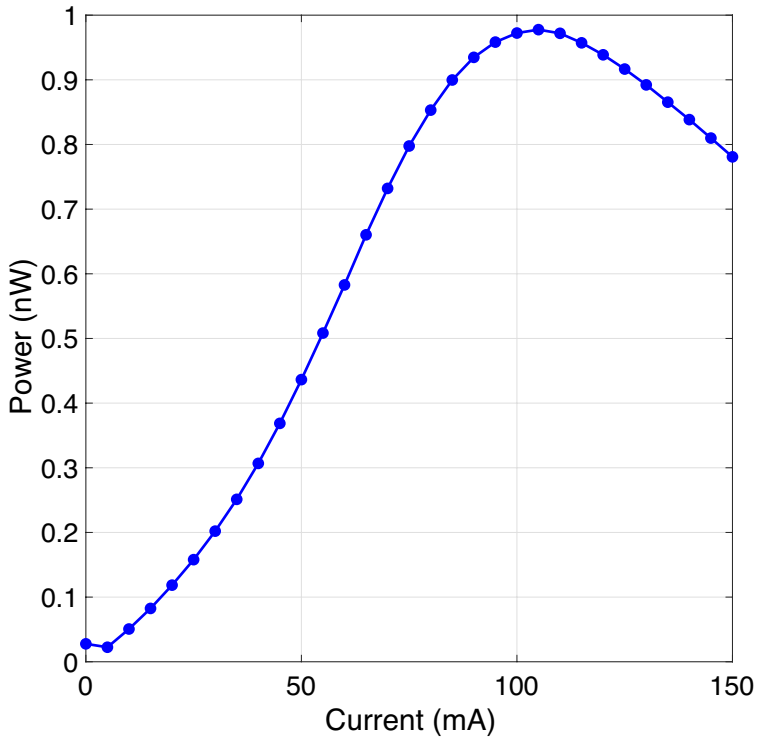

Pulsed

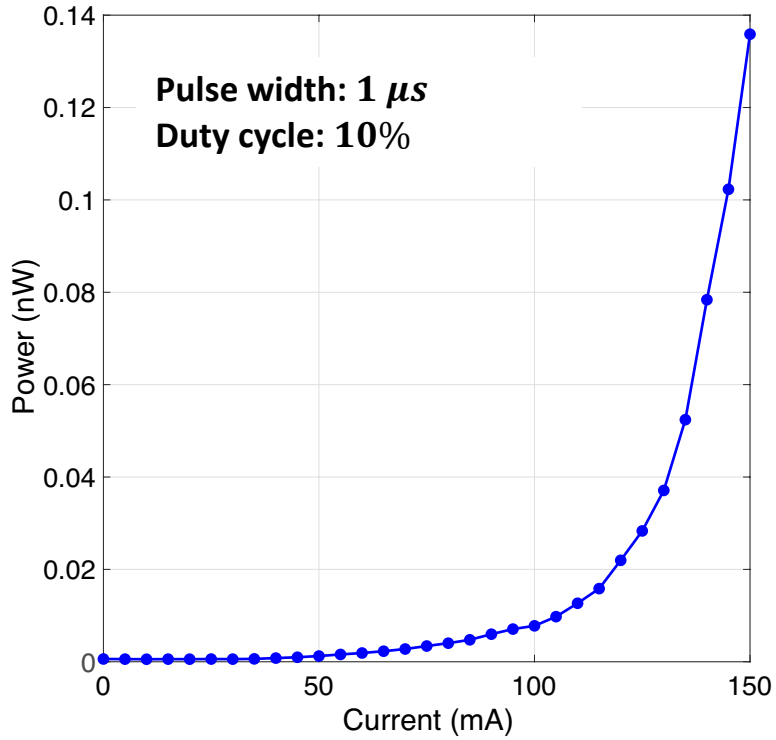

Laser characterization

Caltech

- It was also interesting to check the optical spectrum again under pulsed drive
- On the left and middle panel below are optical spectra taken under pulsed drive at two different average current values. The respective L-I is given on the right below also
- A couple of peaks stand out of the background, the number of which increase upon current increase
- This is clear evidence of lasing, albeit multi-mode and with pretty poor side mode suppression ratio
- It is also worth pointing out that there is no sign of power saturation up to maximum current (300 mA)
- Clearly, overheating is playing a dominant role
- It is also interesting that lasing occurs at ~ 1550 nm, that is, at the TE_0 stopband, which is ~ 30 nm off the gain peak and not near the gain peak itself. This, more than anything else, speaks to the degree of suppression of reflection off the chip facets

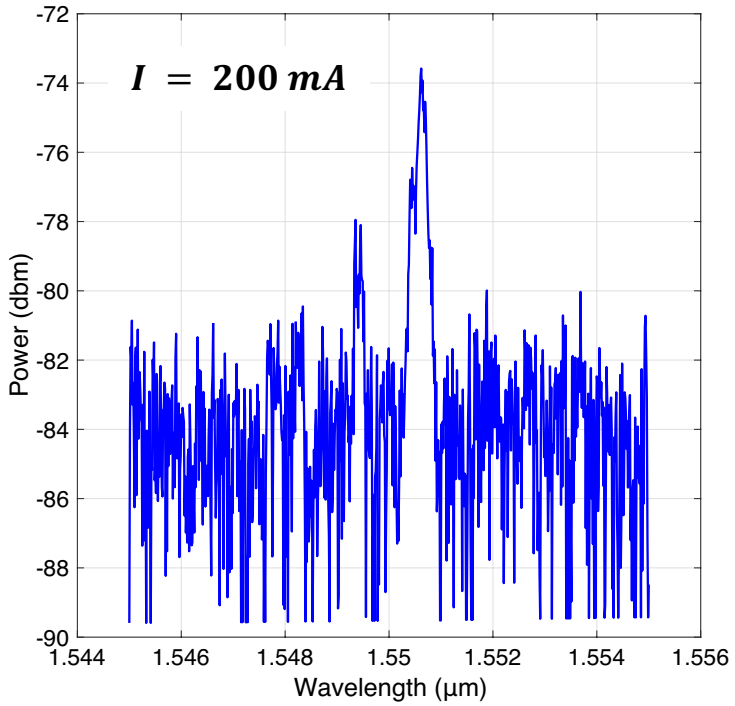

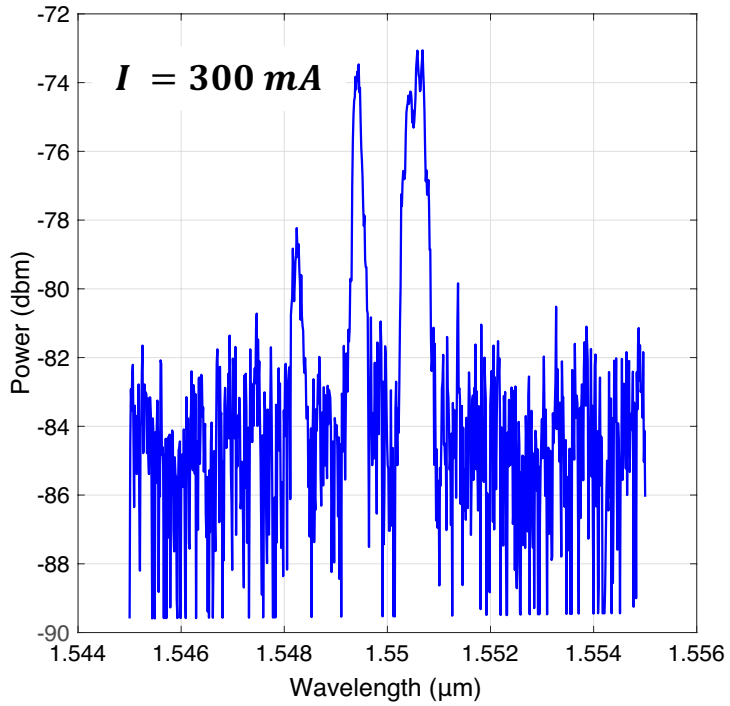

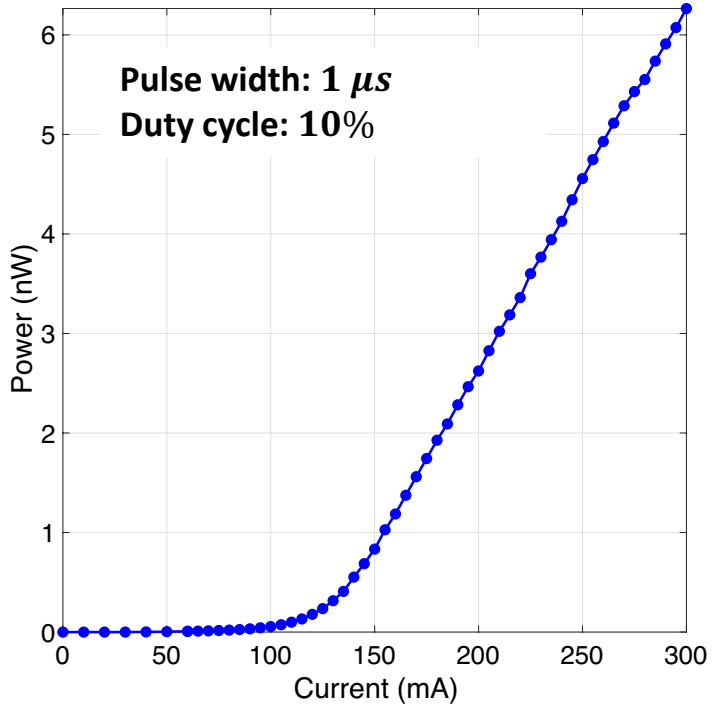

Laser characterization

Caltech

- Out of a few possible options to try and rectify some of the issues with the lasers, we chose to carry out measurements at cryogenic temperatures. Lowering the temperature would cause the gain spectrum to blue-shift, bringing its peak closer to the TE_0 stopband and, thus, increase the probability of CW lasing
- Cryogenic temperature measurements were conducted by MIT-LL. A detailed account can be found in MIT-LL's final report. For completeness, here, we include two examples from those measurements
- On the left below is a plot of L-I and I-V measurements taken at temperatures between 0 and -20^oC. On the right is an optical spectrum measurement for the same device taken at -20^oC. All were taken under CW drive
- Evidence of CW lasing is clear on both the L-I and the optical spectrum. From the latter, the main lasing peak appears at $\sim 1550\ nm$, the location of the TE_0, as expected. Given the resolution bandwidth $(.07\ nm)$ and the laser cavity's FSR $(\sim 12\ GHz)$, it appears the specific laser is oscillating in a single longitudinal mode
- The threshold currents appear significantly reduced from those found for pulsed lasing $(\sim 120\ mA)$ and close to what we theoretically expected for these lasers ($\sim 30\ mA$)
- Output powers remain extremely low (~ 100 uW level) and still saturating, possibly due to overheating

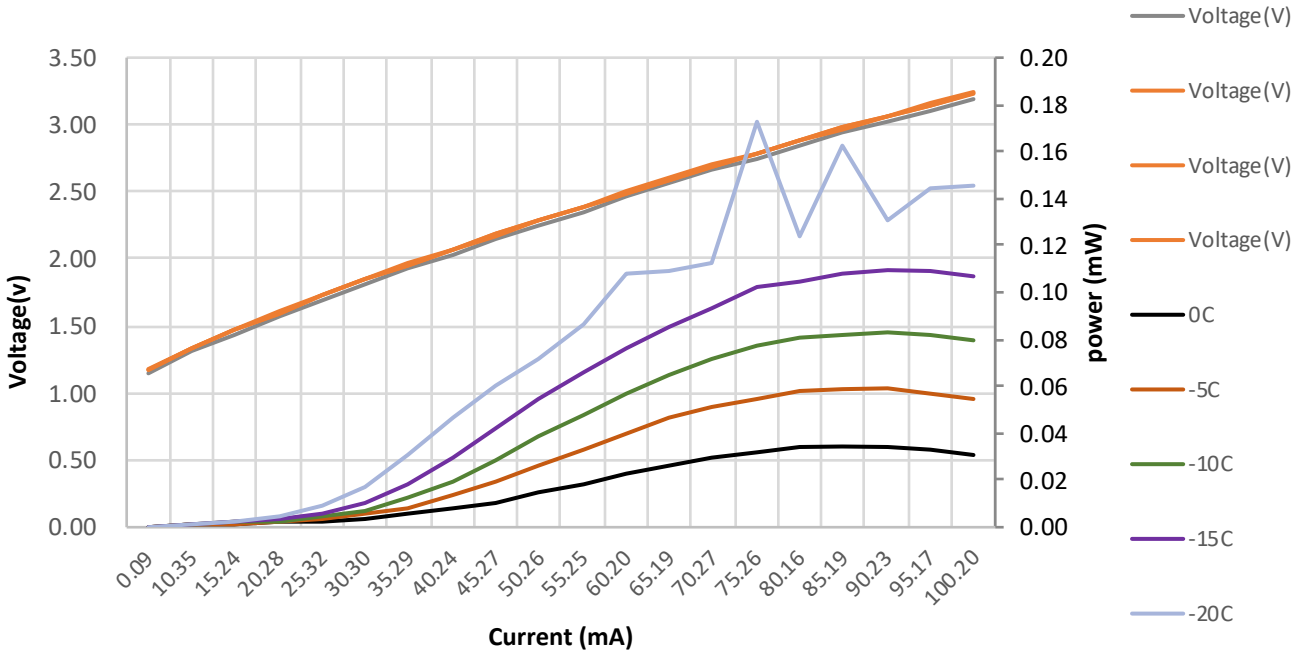

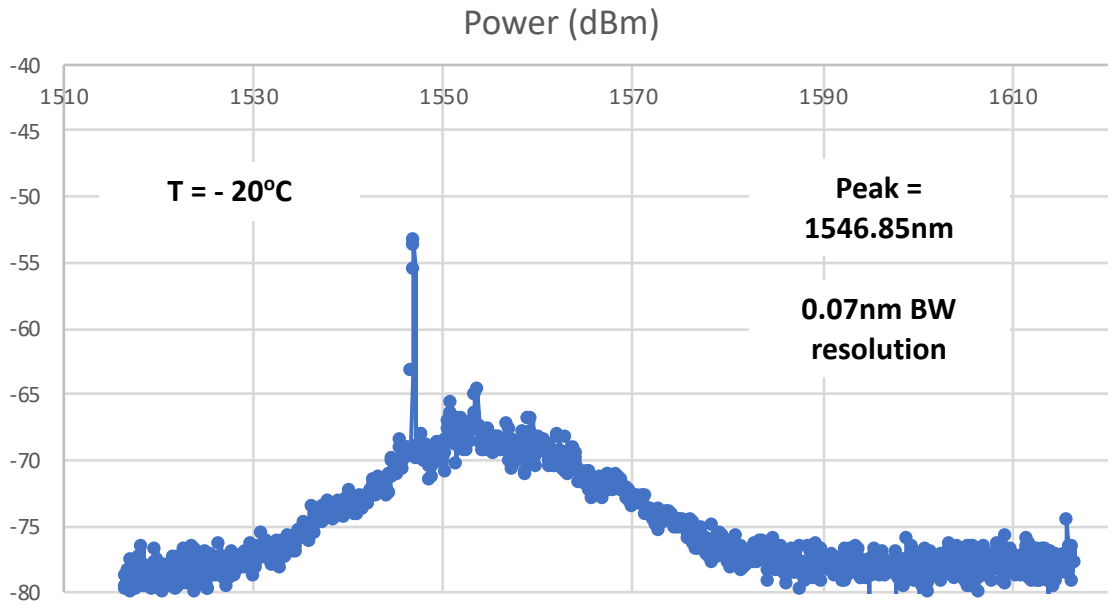

Takeaways and closing thoughts

Caltech

- **There are 2 main factors we attribute the lack of lasing devices, at least CW-RT, to:**
  - Insufficient gain at design wavelength due to large separation between gain peak and grating stopband

    The mismatch between gain peak and stopband is attributed to red-shifting of the gain spectrum under carrier injection relative to its as-grown location. This is known to happen and is, typically, the net result of carrier-induced effects such as bandgap shrinkage and band-filling. It is only moderately and partially offset by a third one, the plasma effect, in the opposite direction (blue-shift). An advance investigation, for example, characterizing F-P lasers with this specific issue in mind, might have helped preempt it by gauging the magnitude of the shift and taking it into account in the grating design
  - Overheating due to higher than expected resistance
- **The biggest challenge in designing the particular laser was ensuring and maintaining single-mode operation**.

  This was, in large part, the result of two, oftentimes, conflicting requirements in terms of target performance; (1) narrow linewidth and, (2) high power, further compounded by inherent, structural peculiarities of the specific device (i.e. ultra-thin, laterally injected III-V). The high sheet resistance, owing to the small III-V thickness, necessitated a significantly longer active region (about 10x longer than ordinary) to keep overall resistance in check, in pursuit of high output power. Doing so, however, increased the spectral density of the longitudinal modes (i.e. smaller FSR), thereby, making mode competition much more close and single-mode oscillation much harder to get and, potentially, more tenuous to maintain. Given what we've learned, were we to do it all over again, we would choose to resolve this conflict by breaking up the problem into two-laser problem or one laser and one amplifier problem. One smaller laser would be responsible for providing a single-frequency, low-power, narrow-linewidth out (by virtue of high-Q). Its output could be amplified to the desired power by an amplifier out of the same active material in tandem, or, used to seed and lock a second, bigger laser in a master-slave configuration
- **Another possible option to simplify the laser design, while still in pursuit of the same performance, would be to reduce the thickness of the III-V further, to no more than $\sim 100\ nm$.**

  Doing so would enable the creation of a mode largely confined in SiN even in the presence of active III-V (QW). This, in turn, would enable a true DFB-type design, inherently single-mode, unlike the present DBR-type. The downside would be potentially more challenging III-V processing and increased sheet resistance.
- Given the novelty of many elements of this laser, as well as its overall complexity, we find that the effort would benefit from a more step-by-step, experiment-driven approach. In the case of this particular project, gits compressed programmatic timeline, coupled with delays, resulted in several novel pieces being brought together all at once and only at the very end, without being rigorously vetted individually in advance.

  For example, characterization of transverse-junction, F-P lasers on native substrate (III-V) could reveal possible issues with the formation the transverse junction and lateral injection process itself. A more thorough characterization of F-P lasers bonded on SiN, especially when contrasted with those on native substrate, could help identify issues created specifically by bonding. The adiabatic mode converter (AMC), one of the more critical elements of this laser, ought to be individually tested and characterized. Indications of adherence issues of the InP taper to the substrate, as well as of excess roughness, suggest that its performance may have been significantly worse than predicted by theory

Final project status and recap

Caltech

	Status	Comments
Tasks		
1. SiN PIC layout & mask tape-out	✓	2x: 1 for Ligentec (800nm) & 1 for MIT-LL (400 nm) SiN
2. III-V/SiN adiabatic mode converter	✓	< .1 db insertion loss (theoretical)
3. High-Q resonator design	✓	2x: Ligentec & MIT-LL SiN
5. Resonator characterization	✓	2x: do-over due to etch depth target miss on 1st run
6. Laser design	✓	Linewidth reduction scheme: frequency locking to high-Q resonator
8. Laser characterization	✓	CW, pulsed L-I, optical spectrum
Performance metrics and milestones		
I. High-Q SiN resonator	✓	$Q_i \sim 2-5\times10^6$ (MIT-LL 400 nm SiN)
II. >20mW output power, >100Hz Lorentzian linewidth	✗	no CW-RT lasing, only pulsed and/or cryo-T
IV. On-chip-powered optical parametric oscillator (i.e. f-comb)	✗	Dropped due to inability to use Ligentec SiN (800 nm)

✓ completed

✗ incomplete

Patent(s)/publications

Caltech

- **Patent(s):** no invention disclosures were made with funds from this grant
- **Publications:** no publications were made, at least by Caltech, pertinent to this project